DIRECT METHANOL FUEL CELLS

JASSIM SULTAN

Your file Votre référence
ISBN: 0-612-89676-5
Our file Notre référence
ISBN: 0-612-89676-5

Direct Methanol Fuel Cells

by

Jassim Sultan

A thesis submitted to the School of Graduate Studies in partial fulfillment of the requirements for the degree of Master of Science.

Department of Chemistry
Memorial University of Newfoundland
St. John's, Newfoundland, Canada
April 2003

For

My

Family

Abstract

This investigation of the characteristics of direct methanol fuel cells (DMFC) has led to significant improvement in their performance. The methanol permeability of Nafion polymer electrolyte membranes has been measured in a DMFC by chronoamperometry. The activation energy for methanol diffusion was determined to be 25 kJ mol^{-1}.

Methanol crossover reduces the performance of the DMFC. Several polypyrrole/Nafion composite membranes were prepared and have been shown to be significantly less permeable to methanol. DMFC performances achieved with some of these polypyrrole/Nafion composite membranes have outperformed those for unmodified Nafion membranes. However, their performances have been shown to be strongly affected by the modification method. Membranes modified by Fe^{3+} oxidation of pyrrole have shown poor bonding with the electrodes, whereas use of H_2O_2 generally yields better results. The performance gains with the composite membranes are due to better cathode activity as a result of methanol crossover reduction.

Acknowledgment

I would like to express my sincerest appreciation to Dr. Peter Pickup for his supervision, guidance and support throughout the duration of my program. My great thanks also to my supervisory committee Dr. Niall Gogan and Dr. Christopher Flinn for their help and comments.

I would also like to thank the members of Dr. Pickup's research group for their help in my research and for the lovely time spent together for the past two years.

Financial support from the School of Graduate Studies, the Chemistry Department, and NSERC are gratefully acknowledged. I would also like to thank H Power Corp. for donation of membranes and electrodes.

Table of Contents

List of Abbreviations

AFC – Alkaline Fuel Cell

CFP – Carbon Fiber Paper

CV – Cyclic Voltammetry or Cyclic Voltammogram

DHE – Dynamic Hydrogen Electrode

DMFC – Direct Methanol Fuel Cell

EDOT – 3,4-ethylenedioxythiophene

EHM – Eisenberg-Hird-Moore model

EIS – Electrochemical Impedance Spectroscopy

EW – Equivalent Weight

MCFC – Molten Carbonate Fuel Cell

MEA – Membrane and Electrode Assembly

NASA – National Aeronautics and Space Administration

OCP – Open Circuit Potential

PAFC – Phosphoric Acid Fuel Cell

PBI – Polybenzimidazole

PEFC – Proton Exchange Fuel Cell

PEM – Polymer Electrolyte Membrane

PTFE – Polytetrafluoroethylene

RHE – Reversible Hydrogen Electrode

SAXS – Small Angle X-ray Scattering

SOFC – Solid Oxide Fuel Cell

SPE – Solid Polymer Electrolyte

List of Tables

List of Figures

Chapter 1

Chapter 3

Chapter 4

Chapter 5

Chapter 1

Introduction

1.1 Introduction to Fuel Cells

Energy is an important requirement to build a modern and developed society. Recently, there is a growing demand for new energy sources that are environmentally friendly as well as highly efficient. Fuel cells have been shown to be an attractive technology to meet these requirements.[1,2]

The invention of the fuel cell was reported in 1839 by Sir William Grove[3] who first presented the alkaline fuel cell. However, Francis Bacon first demonstrated a developed fuel cell device. Bacon's research led to the first application of fuel cells for space flights by the National Aeronautics and Space Administration (NASA) in the 1960s.[4]

A fuel cell can be defined as an instrument that can continuously convert chemical energy to electrical energy through an electrochemical process between an oxidant (fuel) and an oxidizing agent (oxygen from air) using certain types of catalyst.[5] For example, in a hydrogen fuel cell, the hydrogen will be oxidized at the anode, and oxygen will be reduced at the cathode. The half reactions in the fuel cell are as follows (in acid electrolyte):

$$H_2 \longrightarrow 2H^+ + 2e^- \qquad E° = 0.00\ V \quad \textit{Eq. 1.1}$$

$$O_2 + 4H^+ + 4e^- \longrightarrow 2H_2O \qquad E° = 1.23\ V \quad \textit{Eq. 1.2}$$

Fuel cells have several enormous advantages over internal combustion engines. Fuel cells can reduce harmful emissions to zero,[6,7] and protect the environment.[8] Moreover, they can have no (or low) moving parts[9] so noise pollution will be reduced.[10] Theoretically, they are also more efficient;

furthermore, they are relatively safe with mild operation conditions.[11] These attractive advantages have led to widespread and intensive research to improve the performance of fuel cells.

However, with all the bright advantages mentioned above, there are some frustrating difficulties that must be overcome in order to fully commercialize fuel cells. Cost is one of these hurdles and a big barrier to rise above; the catalysts,[12] the membrane (polymer electrolytes)[13] as well as the fuel cell's hardware are expensive. In addition, the volume and the weight of fuel cells is a major defect that should be overcome in certain applications.[14]

There are many different types of fuels cells. The classification can be based on the type of the fuel used, such as: Direct Methanol Fuel Cells (DMFC). Another classification is based on the operating temperature of the fuel cell. There are low temperatures fuel cells, such as: Alkaline Fuel Cells (AFC), Proton Exchange Fuel Cells (PEFC) and Phosphoric Acid Fuel Cells (PAFC). Molten Carbonate Fuel Cells (MCFC) and Solid Oxide Fuel Cells (SOFC) are classified as high temperature fuel cells.[15]

DMFC are the main concern of this thesis. Advantages, limitations, fuel cell design and the characteristics of this type of fuel cell will be discussed in detail. Furthermore, membrane electrolyte, catalysts and methanol electro-oxidation are also among the areas of focus in this thesis.

1.2 Direct Methanol Fuel Cells (DMFC)

1.2.1 Introduction to Direct Methanol Fuel Cells

Direct Methanol fuel cells (DMFC) operate on methanol as a fuel. Methanol is oxidized at the anode to carbon dioxide (CO_2), while oxygen (from air) is reduced at the cathode to water (H_2O). The electrochemical reactions of a DMFC in acid electrolyte occur as follows:

*Anode Reaction:

$$CH_3OH + H_2O \longrightarrow CO_2 + 6H^+ + 6e^- \quad E° = 0.02\ V^{95} \quad \textit{Eq. 1.3}$$

*Cathode reaction:

$$3/2O_2 + 6H^+ + 6e^- \longrightarrow 3H_2O \quad E° = 1.23\ V \quad \textit{Eq. 1.4}$$

*The overall cell reaction:

$$CH_3OH + 3/2\ O_2 \longrightarrow CO_2 + 2H_2O \quad E° = 1.21\ V \quad \textit{Eq. 1.5}$$

Using methanol as a fuel has tremendous advantages relative to hydrogen. Cost is a major incentive for using direct methanol fuel cells. Methanol is a liquid; for that reason it could be easily supplied through the gasoline storage tank infrastructure and allow rapid introduction of fuel cell technology.[16,17] Simple system design and direct liquid feed of methanol into the fuel cell eliminate the processing complexity and safety requirements of hydrogen fuel cells.[18,19,20]

However, direct methanol fuel cells suffer from low power density as a result of slow oxidation kinetics and methanol permeation from the anode compartment to the cathode (crossover).[21,22] Methanol crossover lowers the cathode activity toward oxygen reduction as a result of methanol oxidation. This

causes a mixed potential at the cathode, and therefore lowers the cell potential. Moreover, methanol crossover is responsible for fuel loss.[23,24]

Methanol has been studied as a fuel since the 1950s. As methanol is more reactive in alkaline solution, the first studies used concentrated NaOH or KOH as the electrolyte.[25] A drawback of alkaline electrolytes is carbonate formation as a result of reaction of the electrolyte with carbon dioxide formed from oxidation of methanol. This decreases its conductivity and adds more cost for regeneration. Therefore, several studies used a concentrated sulfuric acid as electrolyte.[25]

However, acid electrolytes suffer form poor performance due to the slow anode reaction which increases the internal resistance of the cell as well as contributing to the corrosion problems of the fuel cell system. In the 1980s, a new promising technology employing polymer electrolyte membranes (PEM) was developed to overcome many of the disadvantages of liquid electrolytes.[26] The desired PEM should have high conductivity, be water insoluble, exhibit good mechanical properties, and have good chemical and thermal stability. In addition, reasonable cost and availability are also requisite.[27,28,29,30]

1.2.2 Design and Characteristics of Direct Methanol Fuel Cells

A schematic diagram of a direct methanol fuel cell (DMFC) system is shown in figure 1.1. The system consists of four major parts: the gas (air or oxygen) supply, the fuel supply system (methanol), a control system to operate

the fuel cell (e.g. pumps, flow meters, temperature controllers, hoses, and electrical connections), and the DMFC itself.

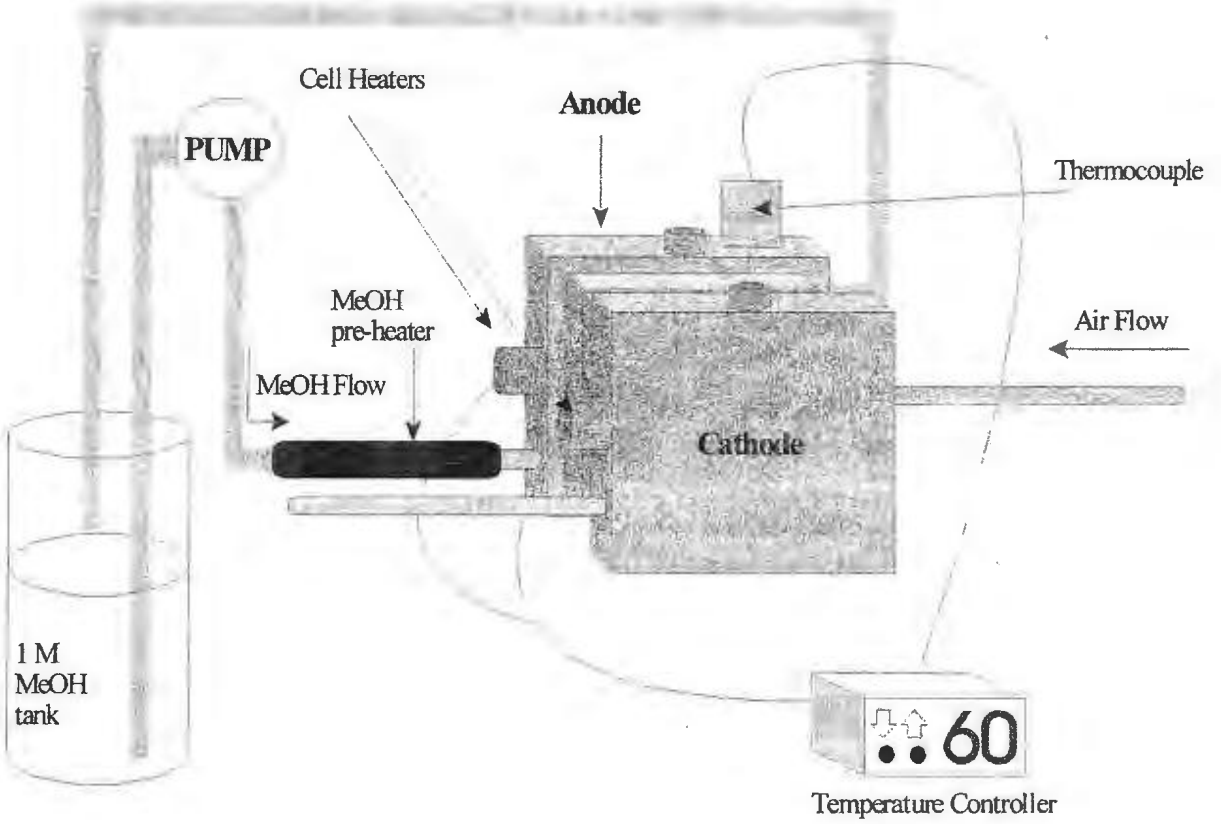

Figure 1.1. A schematic diagram of a direct methanol fuel cell system.

DMFC hardware is constructed mainly from graphite blocks (anode and cathode) with serpentine flow-fields as shown in figure 1.2. The key part of the fuel cell is the membrane and electrode assembly (MEA) which is sandwiched between these blocks by clamping them between two metal plates to seal the cell and support inlet/outlet fittings etc. The methanol (fuel) and the gas (air or

oxygen) are supplied to the MEA through the flow-fields, the geometry and the design of which have a considerable effect on DMFC performance.[31]

Figure 1.2. A schematic diagram of a fuel cell's graphite blocks with serpentine flow-fields.

A schematic diagram of a typical MEA is shown in figure 1.3. It consists of the two electrodes and a polymer electrolyte membrane (PEM), such as Nafion®*. Typically, the MEA is fabricated by a hot pressing procedure, so the catalyst layer is pressed into the Nafion®. The MEA characteristics and structure have a significant effect on the fuel cell performance.[32]

---

*Nafion® is a registered trademark of E.I. du Pont de Nemours & Co.[33]

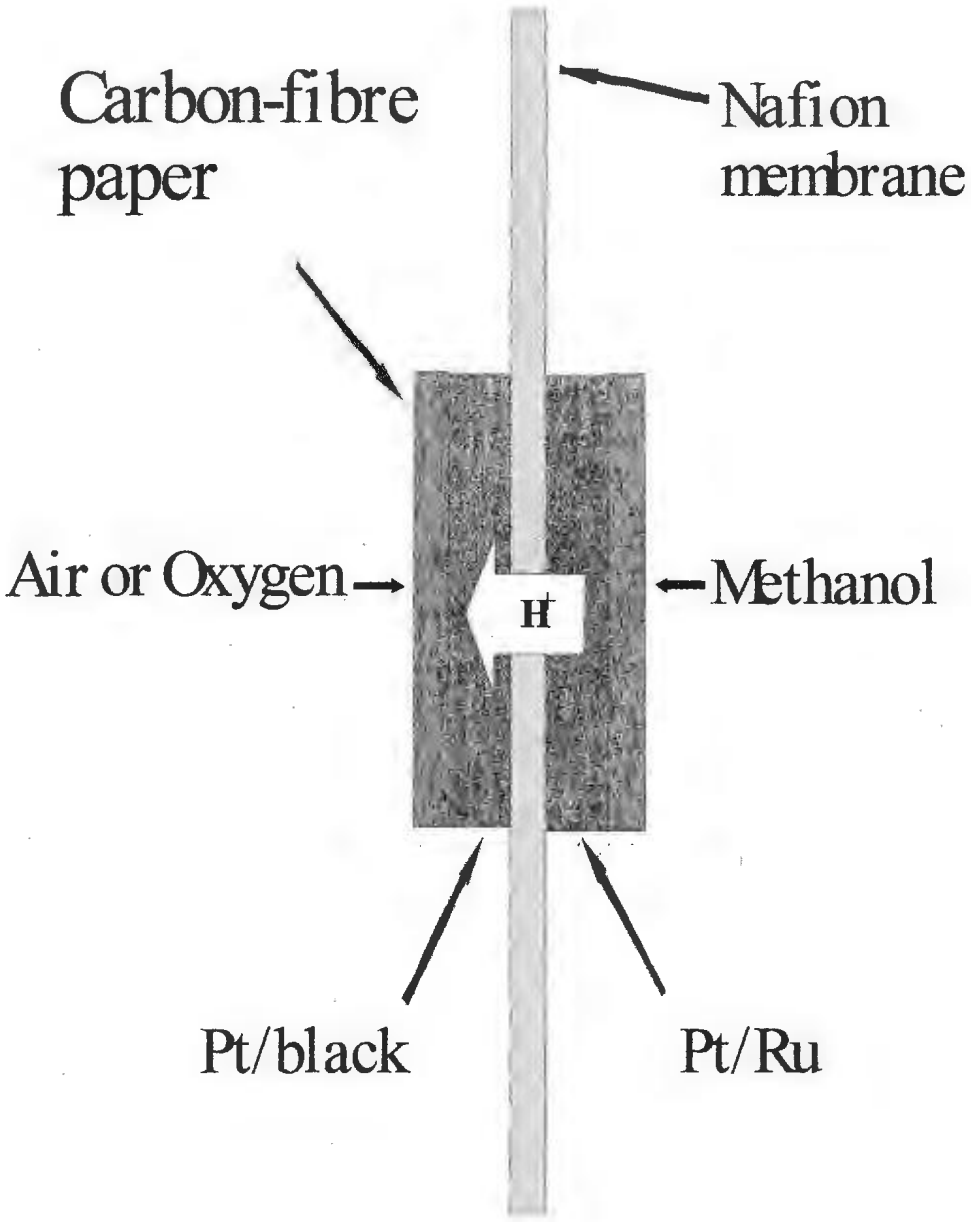

Figure 1.3. A schematic diagram of a membrane and electrode assembly (MEA).

Many factors control the performance of a DMFC. These include the operating conditions, the PEM, and the composition and structure of the catalysts. In addition, methanol crossover is responsible for lowering the efficiency of DMFC performance[34,35,36] (50% loss or more at low current densities).[37]

Thomas *et al.*,[38] have investigated some of the factors that affect the performance of a DMFC. The cell was run at different operating temperatures (80, 100, 110, and 120 °C) with a Pt loading of 2.6 mg cm^{-2}. Figure 1.4 shows a typical example of cell polarization and power density plots of a DMFC at different operating temperatures. Even though a low concentration of methanol (0.5 mol L^{-1}) was used with a flow rate (f_{MeOH}) of 2.0 mL min^{-1}, a peak power density of at least 0.15 W cm^{-2} was obtained at 100 °C.

1.3 Catalysts for Direct Methanol Fuel Cells

1.3.1 Direct Methanol Fuel Cell Anodes

Methanol oxidation occurs through a combination of multi electro-oxidation steps involving several intermediates. Among these species, adsorbed carbon monoxide (CO) is particularly important and problematic. The methanol electro-oxidation process in acid electrolyte involves six electrons per molecule of methanol (see *Eq. 1.3-5*).[39] The best pure metal catalyst for methanol electro-oxidation is Pt.[40]

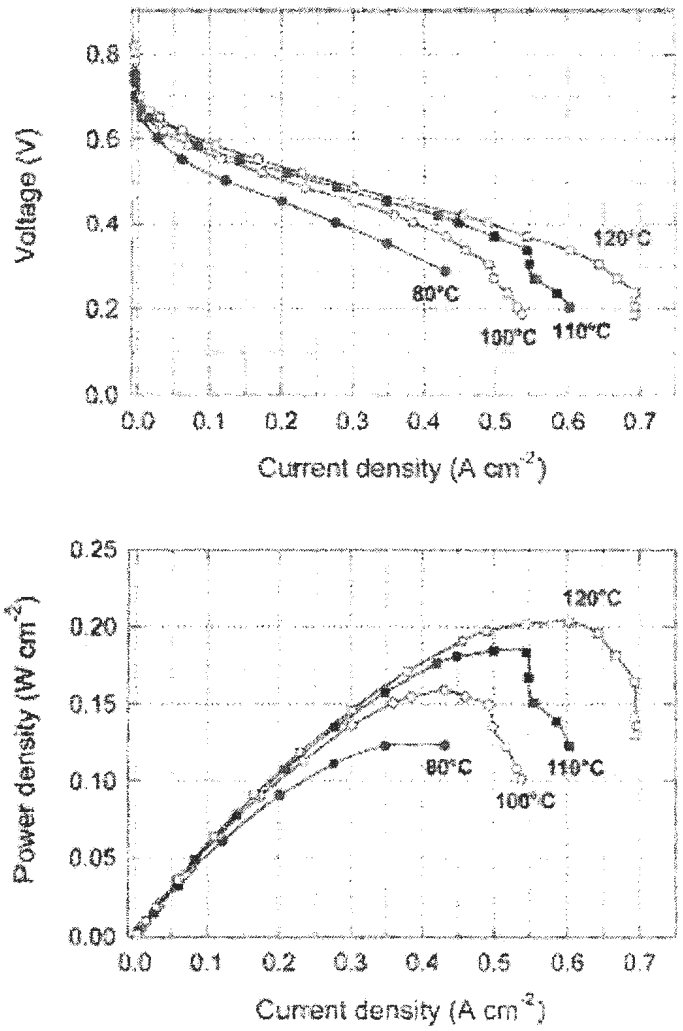

Figure 1.4. Voltage (top) and power density (bottom) as a function of current density for a DMFC with the total Pt loading limited to 2.6 mg cm^{-2}; air cathode at 2.0 *atm* back pressure and high flow stoichiometry; C_{MeOH} = 0.5 M, f_{MeOH}= 2.0 mL min^{-1}.

Reprinted from Thomas, S. C.; Ren, X.; Gottesfeld, S.; Zelenay, P.; *Electrochim. Acta* **2002**, 47, 3744.

CO intermediate species are strongly adsorbed at the surface of Pt and poison the catalyst[41,42] even at extremely low CO concentrations (*ca.* 5-10 ppm).[43] Complete oxidation of CO to CO_2 requires an oxygenated species (e.g. water dissociation, see *Eq. 1.7*) at the Pt surface, however, these species are available only at potentials above *ca.* 0.5 V (vs. RHE) (*Eq.* 1.7).[44,45,46] This potential difference from methanol electro-oxidation which starts to occur at a potential value of *ca.* 0.2 V (vs. RHE)[47] retards the complete oxidation of methanol to CO_2. As a result, poor DMFC performance occurs. For that reason, the CO removal step (water activation) is the rate determining step for methanol electro-oxidation.[48] Increasing the operating temperature of the fuel cell significantly decreases the CO poisoning effect.[49]

The electro-oxidation mechanism is often written as follows:

$$CH_3OH \xrightarrow[\text{(multiple steps)}]{Pt} Pt\text{-}CO_{ads} + 4H^+ + 4e^- \qquad \textit{Eq. 1.6}$$

$$H_2O + Pt \longrightarrow Pt\text{-}OH_{ads} + H^+ + e^- \qquad \textit{Eq. 1.7}$$

$$Pt\text{-}CO_{ads} + Pt\text{-}OH_{ads} \longrightarrow CO_2 + 2Pt + H^+ + e^- \qquad \textit{Eq. 1.8}$$

The poisoning effect of CO on the surface of Pt can be minimized by using various Pt-metal alloy catalysts.[50] Pt-Ru bimetallic catalysts have become the anode of choice for electro-oxidation of methanol.[51] Rolison et al.,[52] claim that a 50:50 atom % Pt-Ru black catalyst has the best performance for methanol electro-oxidation.

The Pt-Ru bimetallic anode decreases the methanol oxidation overpotential by supplying the system with the needed oxygenated species which accelerate oxidation of adsorbed CO to CO_2 at a lower potential of *ca.* 0.2 V (vs. RHE) (*Eq.* 1.9).[44] As a result, DMFC overall performance will be optimized. The Ru function is explained in the following equations:

$$H_2O + Ru \longrightarrow Ru\text{-}OH_{ads} + H^+ + e^- \qquad Eq.\ 1.9$$

From *Eq. 1.6* & *Eq. 1.9*, we obtain:

$$Pt\text{-}CO_{ads} + Ru\text{-}OH_{ads} \longrightarrow CO_2 + Pt + Ru + H^+ + e^- \qquad Eq.\ 1.10$$

Many factors affect the catalytic activity of Pt-Ru anodes, such as the preparation method, structure, morphology, composition, uniformity, dispersion state and alloying state.[53]

1.3.2 Direct Methanol Fuel Cell Cathodes

The cathode activity is very important for DMFC performance. Although the reduction of oxygen is relatively slow (see *Eq. 1.4*), Pt is still the best catalyst for oxygen reduction. In fact, many factors affect the catalytic activity of the cathode. As the methanol fuel is fully miscible with water, it readily crosses over from the anode to the cathode through the polymer electrolyte membrane. At the cathode, it consumes oxygen and can poison the cathode catalyst with carbon monoxide (CO) over time (see section 1.3.1), causing performance losses and a decreased open circuit potential.[54,55]

Moreover, as water is dragged from the anode to the cathode by the proton flux, it may cause flooding of the cathode, which will significantly decrease its activity. Flooding is minimized by increasing the hydrophobicity of the cathode to enhance water removal. Polytetraflouroethylene (PTFE) is incorporated into the catalyst layer to add a hydrophobic characteristic and also act as a binding agent for cathode particles.[56] Water flooding may also be overcome by increasing the flow rate of air (or oxygen), which is, from a design point of view, not desirable as the DMFC system will become more complex.

Pt black is most commonly used as the cathode catalyst. The catalyst is prepared, simply, as an ink-like suspension and then spread over a piece of carbon paper (or carbon cloth) and left to dry. Adding Nafion® to the ink matrix will improve the cathode utilization as it enhances proton conductivity; however, it has poor electron conductivity and low gas diffusion which limit the amount that can be used.[57] Furthermore, the characteristics of the backing layer (carbon paper or cloth) such as thickness, gas permeability and hydrophobic and hydrophilic balance properties of catalysts have an effect on the performance of the fuel cell.

Different types of cathodes are employed in DMFC in addition to Pt black. Carbon supported Pt (Pt/C) cathodes are widely used. Pt alloy cathodes which improve the kinetics for reduction of oxygen are also used.[47]

1.4 Polymer Electrolyte Membranes for Direct Methanol Fuel Cells

The polymer electrolyte membrane (PEM) has two major functions in a direct methanol fuel cell (DMFC). It acts as a solid separator and barrier for the fuel (methanol) and the oxidant gas (air or oxygen), so these membranes are also known as solid polymer electrolytes (SPE). The second function is to be an electrolyte conducting medium for transport of protons (cations) from the anode to the cathode.[58]

A PEM should have certain desired properties to be qualified for fuel cell operation, such as high ionic conductivity, and good chemical and mechanical stability. A feasible price is also a benefit.

This section describes the major types of polymer electrolyte membranes (PEM) that are employed in direct methanol fuel cells.

1.4.1 Perfluorinated Polymer Electrolyte Membranes

Several types of perfluorosulfonated membrane are available under different brand names, such as Nafion®, Flemion®, Aciplex® and Dow®.[59] The one most commonly used in proton exchange fuel cells as a polymer electrolyte membrane is Nafion®,[60,61] a perfluorosulfonic acid polymer developed by E. I. du Pont de Nemours & Co.

The structure of Nafion® is shown in figure 1.5. It consists of a polytetrafluoroethylene (PTFE) backbone with perfluorinated side chains

terminated with sulfonic acid ($-SO_3^-H^+$) groups. The values of x and y are varied to produce membranes with different equivalent weights (EW). EW is the number of grams of polymer per mole of fixed sulfonate groups. These perfluorinated chains endow Nafion® with good mechanical, chemical and thermal stability. Furthermore, they produce water insoluble membranes with high proton conductivity.

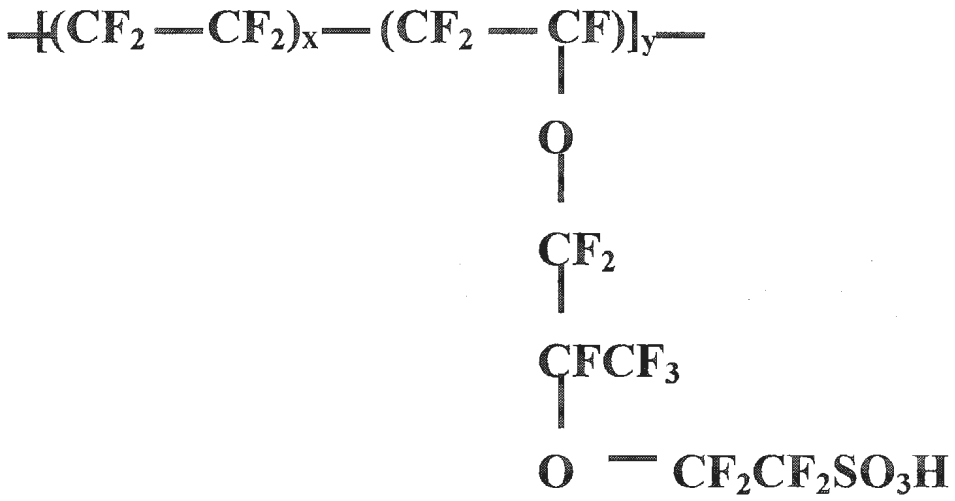

Figure 1.5. The general structure of Nafion®.

These tremendous chemical and physical properties qualify it for many different industrial applications, such as gas separation, gas sensors, electrodialysis, chlor-alkali cells, salt splitting as well as a solid electrolyte membrane in batteries and fuel cells.[62,63]

There are several models to describe the arrangement of ion aggregates within the Nafion® conducting matrix, however, the exact structure is not well

defined.[64] These models include the Yeager Three Phase Model,[65] the Eisenberg-Hird-Moore (EHM) Model of Hydrocarbon Ionomers,[66] the Gierke Cluster Network Model,[67] and the Mauritz-Hopfinger Model.[68]

The Gierke Cluster Network Model describes Nafion® as containing spherical ion clusters (~ 5nm in diameter) bridged by narrow channels (~1nm in diameter). On the other hand, the EHM model proposes that the ionic sites gather together to form multiplets.[69,70] The nano-morphology of Nafion® has been studied using small angle X-ray scattering (SAXS) and through the use of neutron scattering experiments.[71,72] In general, Nafion® membranes consist of the polymer matrix (hydrophobic media), water filled pores (hydrophilic media), and an interfacial zone.[73]

The proton conductivity of Nafion® is highly dependant on the membrane's degree of hydration.[74,75] This drawback of Nafion® limits its operation temperature to below the boiling point of water (i.e. 100 °C at atmospheric pressure), since at high temperature, water evaporation will decrease the water content, resulting in poor membrane conductivity, therefore lowering the fuel cell performance.[76,77] Another limitation of Nafion® membranes is their permeability to methanol[78] which leads to performances losses.

Water has two major sources in a DMFC. In addition to water introduced to the fuel cell system through the aqueous methanol feed, water is also produced as a product of oxygen reduction at cathode. Water transport within the membrane can occur by diffusion under a water concentration gradient, by electo-osmotic

drag when the fuel cell is passing current,[79,80] and by hydraulic permeation when there is a pressure gradient across the membrane.[81]

The properties of Nafion® as a fuel cell membrane can be improved by using composite membranes. For example, Nafion® can be modified by *in situ* polymerization of 1-methylpyrrole[82] or pyrrole,[83] or by forming inorganic/Nafion®[20,84] hybrids.

The high cost of Nafion® opens the door to alternative polymer electrolyte membranes (PEM) with the desired working, chemical and mechanical properties.[85]

1.4.2 Polybenzimidazole Polymer Electrolyte Membranes

The structure of polybenzimidazole (PBI) is shown in figure 1.6. PBI based membranes have high oxidative, mechanical and thermal stability. They are basic with a p*Ka* value of 5.5. Doping of PBI with acids such as phosphoric acid (or sulfuric acid) has enormous positive effects on its conductivity and thermal stability. Delightfully, the acid doped PBI membranes exhibit methanol crossover rates that are ten times less than Nafion®.[86]

Acid doped membranes overcome the high temperature barrier of Nafion®, exhibiting high conductivities at temperatures up to at least 200 °C. Moreover, their electro-osmotic drag coefficient is almost zero.[87] This minimizes water management problems that arise from water transport along with protons from the

anode to the cathode. As a result, the overall performance of the fuel cell is improved.

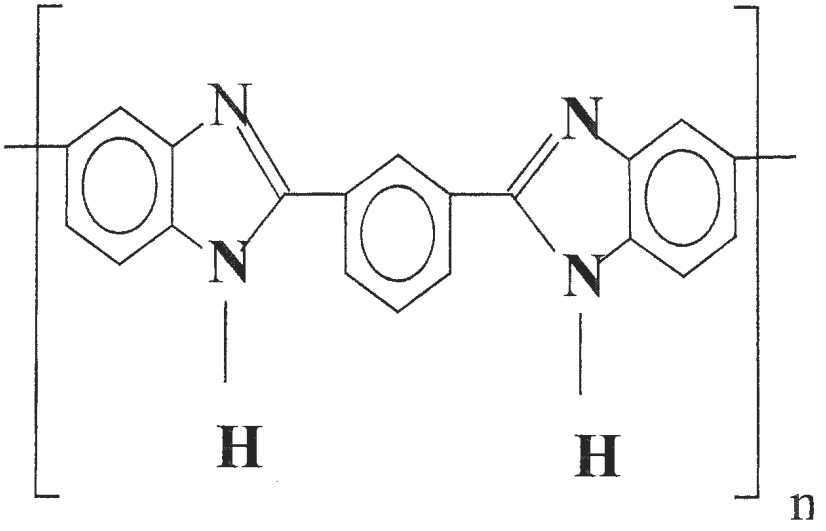

Figure 1.6. The general structure of polybenzimidazole (PBI).

The physical and chemical properties of PBI membranes can be optimized by blending with other polymers. Blending PBI with sulfonated polysulfones increases its thermal stability and enhances its conductivity, besides lowering the cost of the polymer electrolyte membrane.[88,89] These fancy workable properties of PBI membranes, qualify it to be a promising membrane for direct methanol fuel cells.

There are also other different types of PEM with a wide range of properties that are employed in proton exchange fuel cells.[90,91]

1.5 Methanol Electro-Oxidation Mechanisms

Pt-Ru binary anode catalysts have been shown to be the best catalysts for methanol electro-oxidation (see section 1.3.1). The synergistic effect of Pt and Ru has been explained by a bi-functional mechanism. Pt oxidizes methanol through multiple intermediate species to produce Pt-$(CO)_{ads}$ species (see *Eq.* 1.6), on the other hand, Ru provides oxygenated species at lower potentials (see *Eqs.* 1.9-10).[92]

The nature of the intermediate adsorbed species of methanol dehydrogenation is still unknown and they have not been identified clearly. However, Hirose *et al.*,[93] reported that, besides CO species, there are also formate species on Pt. Another study claimed the formation of formaldehyde and formic acid species.[94,95]

Goddard *et al.*,[96] suggested a mechanism for methanol electro-oxidation using Pt-Ru alloy anode catalysts involving successive oxidation steps. Methanol molecules will be adsorbed at the surface of Pt then undergo successive oxidation half reactions ending with CO_{ads} species, as shown through *Eqs.*1.11-14:

$$(CH_3OH)_{ads} \longrightarrow (CH_3O)_{ads} + H^+ + e^- \qquad \textit{Eq.}\ 1.11$$

$$(CH_3O)_{ads} \longrightarrow (CH_2O)_{ads} + H^+ + e^- \qquad \textit{Eq.}\ 1.12$$

$$(CH_2O)_{ads} \longrightarrow (CHO)_{ads} + H^+ + e^- \qquad \textit{Eq.}\ 1.13$$

$$(CHO)_{ads} \longrightarrow (CO)_{ads} + H^+ + e^- \qquad \textit{Eq.}\ 1.14$$

Ru dissociates water at lower overpotentials than Pt alone and supplies the system with the required oxygenated species at a faster rate (Eqs. 1.15-16), thus

decreasing the concentration of CO_{ads} species and improving the performance of fuel cell.

$$(H_2O)_{ads} \longrightarrow (OH)_{ads} + H^+ + e^- \qquad Eq.\ 1.15$$

$$(OH)_{ads} \longrightarrow (O)_{ads} + H^+ + e^- \qquad Eq.\ 1.16$$

The oxidation of water to O_{ads} and methanol to CO_{ads} and their combination according to *Eq.* 1.17 leads to the formation of CO_2:

$$(CO)_{ads} + (O)_{ads} \longrightarrow CO_2 \qquad Eq.\ 1.17$$

The equations mentioned previously (Eqs. 1.11-17) assume there are no side reactions, however, a possible combination pathway between *Eq.* 1.14 and *Eq.* 1.15 to obtain *Eq.* 1.18:

$$(CO)_{ads} + (OH)_{ads} \longrightarrow (COOH)_{ads} \longrightarrow CO_2 + H_{ads} \qquad Eq.\ 1.18$$

The role of Ru is significant, as it will enhance the oxidation of CO to CO_2 through water decomposition at a lower voltage (~ 0.2 V vs. RHE), which is lower than pure Pt (above 0.5 V vs. RHE).

1.6 Thesis Objectives

The main goals of this thesis are to understand and study the factors that influence the performance of a DMFC and to improve and modify it.

Chapter three of this thesis investigates the permeability properties of Nafion® membranes. Methanol crossover properties were studied over a range of temperatures (from near room temperature up to 60 °C) and concentrations. The affect of membrane thickness on methanol crossover was also explored.

Modification of Nafion membranes by *in situ* polymerization with conducting polymers are showing promising results on DMFC performance, as these composite membranes decrease the methanol crossover. Chapter four describes the methods used for modification and characterization of these modified membranes, and their performance in a DMFC.

Finally, chapter five analyses the effects of the modified membranes on the anode and cathode activity using electrochemical impedance spectroscopy (EIS).

References

[1] Broka, K.; Ekdunge, P.; *J. Appl. Electrochem.* **1997**, 27, 281-289.

[2] Qingfeng, L.; Hjuler, H. A.; Hasiotis, C.; Kallitsis, J. K.; Kontoyannis, C. G.; Bjerrum, N. J.; *Electrochem. Solid-State Lett.* **2002**, 5, 6, A125-A128.

[3] Grove, W. R.; *Philos. Mag.* **1839**, 14, 127.

[4] De Geeter, E.; Mangan, M.; Spaepen, S.; Stinissen, W.; Vennekens, G.; *J. Power Sources* **1999**, 80, 207-212.

[5] Zhu, B.; Meng, G.; Mellander, B.-E.; *J. Power Sources* **1999**, 79, 30-36.

[6] Chu, D.; Jiang, R.; *J. Power Sources* **1999**, 80, 226-234.

[7] Gutmann, G.; *J. Power Sources* **1999**, 84, 275-279.

[8] Miyake, N.; Wainright, J. S.; Savinell, R. F.; *J. Electrochem. Soc.* **2001**, 148, 8, A905-A909.

[9] Adjemian, K. T.; Lee, S. J.; Srinivasan, S.; Benziger, J.; Bocarsly, A. B.; *J. Electrochem. Soc.* **2002**, 149, 3, A256-A261.

[10] Kordesch, K. V.; Simader, G. R.; *Chem. Rev.* **1995**, Vol. 95, No. 1, 191-201.

[11] Marr, C.; Li, X.; *ARI* **1998**, 50, 190-200.

[12] Perry, M. L.; Fuller, T. F.; *J. Electrochem. Soc.* **2002**, 149, 7, S59-S67.

[13] Kreuer, K. D.; *J. Membr. Sci.* **2001**, 185, 29-39.

[14] Buchi, F. N.; Srinivasan, S.; *J. Electrochem. Soc.* **1997**, Vol. 144, No. 8, 2767-2772.

[15] Carrette, L.; Friedrich, K. A.; Stimming, U.; *ChemPhysChem* **2000**, 1, 162-193.

[16] Shulka, A. K.; Ravikumar, M. K.; Gandhi, K. S.; *J. Solid State Electrochem.* **1998**, 2, 117-122.

[17] Baldauf, M.; Preidel, W.; *J. Power Sources* **1999**, 84, 161-166.

[18] Gonzalez, M. J.; Peters, C. H.; Wrighton, M. S.; *J. Phys. Chem. B* **2001**, 105, 5470-5476.

[19] Uchida, H.; Mizuno, Y.; Watanabe, M.; *J. Electrochem. Soc.* **2002**, 149, 6, A682-A687.

[20] Yang, C.; Srinivasan, S.; Arico, A. S.; Creti, P., Baglio, V.; Antonucci, V.; *Electrochem. Solid-State Lett.* **2001**, 4, 4, A31-A34.

[21] Jusys, Z.; Behm, R. J.; *J. Phys. Chem. B* **2001**, 105, 10874-10883.

[22] Ren, X.; Springer, T. E.; Gottesfeld, S.; *J. Electrochem. Soc.* **2000**, 147, 1, 92-98.

[23] Heinzel, A.; Barragan, V. M.; *J. Power Sources* **1999**, 84, 70-74.

[24] Kauranen, P. S., Skou, E.; *J. Appl. Electrochem.* **1996**, 26, 909-917.

[25] Lamy, C.; Léger, J-M.; Srinivasan, S.; *Modern Aspects of Electrochemistry*, No. 34, Bockris, J. O'M; Conway, B. E., Eds; Kluwer Academic/Plenum Publishers: New York, **2001**, pp 53-118.

[26] Shukla, A. K., Christensen, P. A.; Dickinson, A. J.; Hamnett, A.; *J. Power Sources* **1998**, 76, 54-59.

[27] Gautier-Luneau, I.; Denoyelle, A.; Sanchez, J. Y.; Poinsignon, C.; *Electrochim. Acta* **1992**, Vol. 37, No. 9, pp. 1615-1618.

[28] Beattie, P. D.; Orfino, F. P.; Basura, V., I.; Zychowska, K.; Ding, J.; Chuy, C.; Schmeisser, J.; Holdcroft, S.; *J. Electroanal. Chem.* **2001**, 503, 45-56.

[29] Norby, T.; *Solid State Ionics* **1999**, 125, 1-11.

[30] Yamaguchi, T.; Ibe, M.; Nair, B. N.; Nakao, S.-I.; *J. Electrochem. Soc.* **2002**, 149, 11, A1448-A1453.

[31] Amphlett, J. C.; Peppley, B. A.; Halliop, E.; Sadiq, A.; *J. Power Sources* **2001**, 96, 204-213.

[32] Arico, A. S.; Creti, P.; Antonucci, P. L.; Cho, J.; Kim, H.; Antonucci, V.; *Electrochim. Acta* **1998**, Vol. 43, No. 24, 3719-3729.

[33] Wintersgill, M. C.; Fontanella, J.; *Electrochim. Acta* **1998**, Vol. 43, Nos. 10-11, 1533-1538.

[34] Walker, M.; Baumgartner, K.-M.; Kaiser, M.; Kerres, J.; Ullrich, A.; Rauchle, E.; *J. Appl. Polym. Sci.* **1999**, Vol. 74, 67-73.

[35] Skou, E.; Kauranen, P.; Hentschel, J.; *Solid State Ionics* **1997**, 97, 333-337.

[36] Mench, M. M.; Wang, C. Y.; *J. Electrochem. Soc.* **2003**, 150, 1, A79-A85.

[37] Muller, J. T.; Urban, P. M.; Holderich, W. F.; Colbow, K. M.; Zhang, J.; Wilkinson, D. P.; *J. Electrochem. Soc.* **2000**, 147, 11, 4058-4060.

[38] Thomas, S. C.; Ren, X.; Gottesfeld, S.; Zelenay, P.; *Electrochim. Acta* **2002**, 47, 3741-3748.

[39] Zhu, Y.; Cabrera, C. R.; *Electrochem. Solid-State Lett.* **2001**, 4, 4, A45-A48.

[40] Gojkovic, S. L.; Vidakovic, T. R.; *Electrochim. Acta* **2001**, 47, 633-642.

[41] Wang, Y.; Fachini, E. R.; Cruz, G.; Zhu, Y.; Ishikawa, Y.; Colucci, J. A.; Cabrera, C. R.; *J. Electrochem. Soc.* **2001**, 148, 3, C222-C226.

[42] Ciureanu, M.; Wang, H.; Qi, Z.; *J. Phys. Chem. B* **1999**, 103, 9645-9657.

[43] Nakajima, H.; Nomura, S.; Sugimoto, T.; Nishikawa, S.; Honma, I.; *J. Electrochem. Soc.* **2002**, 149, 8, A953-A959.

[44] Hoster, H.; Iwasita, T.; Baumgartner, H.; Vielstich, W.; *J. Electrochem. Soc.* **2001**, 148, 5, A496-A501.

[45] Melnick, R. E.; Palmore, G. T. R.; *J. Phys. Chem.* **2001**, 105, 1012-1025.

[46] Melnick, R. E.; Palmore, G. T. R; *J. Phys. Chem. B* **2001**, 105, 9449-9457.

[47] Arico, A. S.; Srinivasan, S.; Antonucci, V.; *Fuel Cells* **2001**, 1, No. 2, 133-161.

[48] Bo, A.; Sanicharane, S.; Sompalli, B.; Fan, Q.; Gurau, B.; Liu, R.; Smotkin, E. S.; *J. Phys. Chem. B* **2000**, 104, 7377-7381.

[49] Honma, I.; Nakajima, H.; Nishikawa, O.; Sugimoto, T.; Nomura, S.; *J. Electrochem. Soc.* **2002**, 149, 10, A1389-A1392.

[50] Steigerwalt, E. S.; Deluga, G. A.; Cliffel, D. E.; Lukehart; *J. Phys. Chem. B* **2001**, 105, 8097-8101.

[51] Liu, Y.-C.; Qiu, X.-P.; Huang, Y.-Q.; Zhu, W.-T.; *J. Power Sources* **2002**, 111, 160-164.

[52] Rolison, D. R.; Hagans, P. L.; Swider, K. E.; Long, J. W.; *Langmuir* **1999**, 15, 774-779.

[53] Takasu, Y.; Fujiwara, T.; Murakami, Y.; Sasaki, K.; Oguri, M.; Asaki, T.; Sugimoto, W.; *J. Electrochem. Soc.* **2000**, 147, 12, 4421-4427.

[54] Hobson, L. J.; Ozu, H.; Yamaguchi, M.; Hayase, S.; *J. Electrochem. Soc.* **2001**, 148, 10, A1185-A1190.

[55] Shao, Z.-G.; Hsing, I-M.; *Electrochem. Solid-State Lett.* **2002**, 5, 9, A185-A187.

[56] Giorgi, L.; Antolini, E.; Pozio, A.; Passalacqua, E.; *Electrochim. Acta* **1998**, Vol. 43, No. 24, 3675-3680.

[57] Easton, E. B.; Qi, Z.; Kaufman, A.; Pickup, P. G.; *Electrochem. Solid-State Lett.* **2001**, 4, 5, A59-A61.

[58] Ding, J.; Chuy, C.; Holdcroft, S.; *Chem. Mater.* **2001**, Vol. 13, No. 7, 2231-2233.

[59] Baradie, B.; Dodelet, J. P.; Guay, D.; *J. Electroanal. Chem.* **2000**, 489, 101-105.

[60] Doyle, M.; Choi, S. K.; Proulx, G.; *J. Electrochem. Soc.* **2000**, 147, 1, 34-37.

[61] Buchi, F.; Scherer, G. G.; *J. Electrochem. Soc.* **2001**, 148, 3, A183-A188.

[62] Ren, X.; Springer, T. E.; Zawodzinski, T. A.; Gottesfeld, S.; *J. Electrochem. Soc.* **2000**, 147, 2, 466-474.

[63] Slade, S.; Campbell, S. A.; Ralph, T. R.; Walsh, F. C.; *J. Electrochem. Soc.* **2002**, 149, 12, A1556-A1564.

[64] Anantaraman, A. V.; Gardner, C. L.; *J. of Electroanal. Chem.* **1996**, 414, 115-120.

[65] Yeager, H. L.; Steck, A.; *J. Electrochem. Soc.* **1981**, Vol. 128, No. 9, 1880-1884.

[66] Eisenberg, A.; Hird, B.; Moore, R. B.; *Macromolecules* **1990**, 23, 4098.

[67] Gierke, T. D.; Munn, G. E.; Wilson, F. C.; *J. Polym. Sci. Polym. Phys. Ed.* **1981**, 19, 1687.

[68] Mauritz, K. A.; Hora, C. J.; Hopfinger, A. J. in: *Ions in Polymers*; ed. A. Eisenberg, ACS Advance in Chemistry Ser. No. 187, American Chemical Society: Washington, DC, **1980**, pp. 124-154.

[69] Zawodzinski JR, T. A.; Springer, T. E.; Urbi, F.; Gottesfeld, S.; *Solid State Ionics* **1993**, 60, 199-211.

[70] Ding, J.; Chuy, C.; Holdcroft, S.; *Macromolecules* **2002**, 35, 1348-1355.

[71] Haubold, H.-G.; Vad, T.; Jungbluth, H.; Hiller, P.; *Electrochim. Acta* **2001**, 46, 1559-1563.

[72] Orfino, F. P.; Holdcroft, S.; *J. New Mater. Electrochem. Syst.* **2000**, 3, 285-290.

[73] Rollins, H. W.; Lin, F.; Johnson, J.; Ma, J.-J.; Liu, J.-T.; Tu, M.-H.; DesMarteau, D. D.; Sun, Y.-P.; *Langmuir* **2000**, 16, 8031-8036.

[74] Cappadonia, M.; Erning, J. W.; Niaki, S. M. S.; Stimming, U.; *Solid State Ionics* **1995**, 77, 65-69.

[75] Okada, T.; Xie, G.; Gorseth, O., Kjelstrup, S.; Nakamura, N.; Arimura, T.; *Electrochim. Acta* **1998**, Vol. 43, No. 24, 3741-3747.

[76] Miyake, N.; Wainright, J. S.; Savinell, R. F.; *J. Electrochem. Soc.* **2001**, 148, 8, A898-A904.

[77] Costamagna, P.; Yang, C.; Bocarsly, A. B.; Srinivasan, S.; *Electrochim. Acta* **2002**, 47, 1023-1033.

[78] Carter, R.; Wycisk, R.; Yoo, H., Pintauro, P. N.; *Electrochem. Solid-State Lett.* **2002**, 5, 9, A195-A197.

[79] Ren, X., Henderson, W.; Gottesfeld, S.; *J. Electrochem. Soc.* **1997**, Vol. 144, No. 9, L267-L270.

[80] Zawodzinski Jr., T. A.; Derouin, C.; Radzinski, S.; Sherman, R. J.; Smith, V. T.; Springer, T. E.; Gottesfeld, S.; *J. Electrochem. Soc.* **1993**, Vol. 140, No. 4, 1041-1047.

[81] Ren, X.; Gottesfeld, S.; *J. Electrochem. Soc.* **2001**, 148, 1, A87-A93.

[82] Jia, N., Lefebvre, M. C.; Halfyard, J.; Qi, Z.; Pickup, P.G.; *Electrochem. Solid-State Lett.* **2000**, 3, 12, 529-531.

[83] E. B. Easton, Ph.D. Thesis, Memorial University of Newfoundland, St. John's, Newfoundland, Canada (2003).

[84] Mauritz, K. A.; Stefanithis, I. D.; Davis, S. V.; Scheetz, R. W.; Pope, R. K.; Wilkes, G. L.; Huang, H-H.; *J. Appl. Polym. Sci.* **1995**, 55, 181-190.

[85] Kerres, J.; Ullrich, A.; Meier, F.; Haring, T.; *Solid State Ionics*, **1999**, 125, 243-249.

[86] Wang, J.-T.; Wainright, J. S.; Savinell, R. F.; Litt, M.; *J. Appl. Electrochem.* **1996**, 26, 751-756.

[87] Wang, J.-T.; Savinell, R. F.; Wainright, J.; Litt, M.; Yu, H.; *Electrochim. Acta* **1996**, Vol. 41, No. 2, pp 193-197.

[88] Hasiotis, C.; Qingfeng, L.; Deimede, V.; Kallitsis, J. K.; Kontoyannis, C. G.; Bjerrum, N. J.; *J. Electrochem. Soc.* **2001**, 148, 5, A513-A519.

[89] Deimede, V.; Voyiatzis, G. A.; Kallitsis, J. K.; Qingfeng, L.; Bjerrum; *Macromolecules* **2000**, 33, 7609-7617.

[90] Guo, X.; Fang, J.; Watari, T.; Tanaka, K.; Kita, H.; Okamoto, K.-I.; *Macromolecules* **2002**, 35, 6707-6713.

[91] Savadogo, O.; *J. New Mater. Electrochem. Syst.* **1998**, 1, 47-66.

[92] Long, J. W.; Stroud, R. M.; Swider-Lyons, K. E.; Rolison, D. R.; *J. Phys. Chem. B* **2000**, 104, 9772-9776.

[93] Endo, M.; Matsumoto, T.; Kubota, J.; Domen, K.; Hirose, C.; *J. Phys. Chem. B* **2001**, 105, 1573-1577.

[94] Lu, G.-Q.; Chrzanowski, W.; Wieckowski, A.; *J. Phys. Chem. B* **2000**, 104, 5566-5572.

[95] Iwasita, T.; *Electrochim. Acta* **2002**, 47, 3663-3674.

[96] Kua, J.; Goddard, W. A.; *J. Am. Chem. Soc.* **1999**, 121, 10928-10941.

Chapter 2

Chemicals, Instrumentation and Methods

2.1 Chemicals

All chemicals and gases (N_2, O_2, and air) were used as commercially delivered without any pretreatment. All aqueous solutions were prepared from distilled and deionized water.

2.2 Electrochemical Instruments

2.2.1 EG&G PAR 273A Potentiostat/Galvanostat and 5210 Lock-in Amplifier

These instruments were used for measuring current/voltage curves (polarization, CV, etc.) for the direct methanol fuel cell. All data were collected and experiments controlled by EG&G/PAR 270A electrochemical software. Electrochemical Impedance Spectra (EIS), on the other hand, were collected by PAR Powersuit software.

2.2.2 Direct Methanol Fuel Cell

All experiments were performed on a commercial 5.29 cm^2 fuel cell sold by ElectroChem. Inc. and constructed from electrochemical grade graphite blocks with serpentine flow-fields. A schematic diagram of these blocks is shown previously in figure 1.2.

2.3 Membrane Electrolyte Assembly (MEA) Preparation

2.3.1 Nafion® cleaning procedure

Unless stated otherwise, all the cleaning solutions were hot (close to boiling point). Nafion® pieces or sheets were cleaned in hot 15% H_2O_2 solution for at least one hour (until the membranes were transparent and colorless, which sometimes required more than one hour).

The clean membranes were then soaked in hot 1 mol L^{-1} nitric acid (HNO_3) solution for another one hour, and then soaked in hot 1 mol L^{-1} sulfuric acid (H_2SO_4) for also one hour. The last step is to soak the membrane in hot water for at least 1 hour to remove the excess acid. The membranes were washed with water between each cleaning step. Finally, the clean membranes were stored in water at room temperature.

2.3.2 MEA Preparation

All MEAs were assembled by a hot pressing procedure, using a Carver Laboratory Press (model M) equipped with two heating elements (Carver model 2102-1).

A 5.29 cm^2 home made die was used to simplify the process and to align the electrodes. The pressing temperature was 130 °C, under a force of 500 pounds for a time period of 90-180 seconds, unless otherwise specified.

2.4 Testing of MEAs

The DMFC experiments were performed at different concentrations of methanol (0.1, 0.3, 0.6, 1.0 mol L^{-1}). The methanol solution was supplied to the DMFC from a micro-mate interchangeable 50 mL syringe (Perfektum®, Popper & Sons, Inc.) using a compact infusion pump model No. 975 (Harvard Apparatus Co., Inc.), equipped with a changeable flow rate drive. Gases were supplied directly from the tanks with the inlet flow rate controlled by a Cole Parmer (model NO 42-15) flow meter.

The temperature of the DMFC was controlled by a Cole Parmer Co. temperature controller (model BA-2155-54). The temperature of the DMFC was allowed to stabilize for about 30-45 minutes before any experiments.

The DMFC was operated with either oxygen or air passing through the cathode to obtain polarization curves. Polarization readings were measured by applying a constant current from the potentiostat/galvanostat. Voltage readings were recorded after a stabilization time of 3 minutes to achieve a stable and a steady value.

Chronoamperometric experiments were performed to measure methanol crossover. Nitrogen (N_2) gas was passed through the cathode compartment instead of oxygen (or air) and the potential of the DMFC cathode was stepped to values in the range of +0.7 to +0.9 V vs the DMFC anode (see section 3.3.1). As methanol crosses through the membrane to the fuel cell cathode which acts as an anode under these conditions, it is oxidized to produce carbon dioxide. Hydrogen gas

(H_2) is evolved at the fuel cell anode, which acts as a cathode under these conditions and then behaves as a dynamic hydrogen electrode (DHE). The limiting current for methanol oxidation (crossover) was recorded by averaging the last 40 seconds of the current vs time curve.

2.5 Presentation of Data

Throughout this thesis, lines are drawn through data points as an aid to visualization.

Chapter 3

Characterization of Methanol Crossover through Nafion® Membranes

3.1 Introduction

Methanol is introduced directly to a DMFC as an aqueous solution. As methanol is fully miscible with water, it readily crosses over from the anode to the cathode compartment through the hydrated Nafion® membrane. This characteristic of PEM DMFCs is responsible for fuel losses and reducing the cathode catalytic activity over time, causing performance losses and a decreased open circuit potential.[1,2] Methanol crossover lowers the cathode activity towards oxygen reduction as a result of methanol oxidation which results in the formation of CO species which poison the Pt catalyst. This causes a mixed potential at the cathode.[3]

Methanol permeation is one of the challenging problems affecting DMFC performance and many groups have investigated methanol transport.[4] Methanol crossover can be monitored and determined indirectly by measuring the amount of CO_2 produced at the cathode as a result of methanol oxidation. CO_2 gas emission can be measured by electrochemical methods,[5,6] by IR-detector methods[7,8] and by chromatographic analysis.[9]

A schematic diagram showing the electrochemical measurement of the methanol permeation process is shown in figure 3.1. Methanol crosses from the anode through the membrane to the cathode, which is operated under an inert environment by passing nitrogen gas through the cathode compartment. Under these conditions, methanol is oxidized to produce carbon dioxide. Hydrogen gas is evolved at the fuel cell anode, which serves as a cathode under these conditions

and behaves as a dynamic hydrogen electrode (DHE). The membrane permeability (P) is a function of the limiting current density (I_{lim}) and can be calculated from the following equation:

$$P = C_m D_m = I_{lim} \frac{d}{nFK_{dl}} \qquad \textit{Eq. 3.1}$$

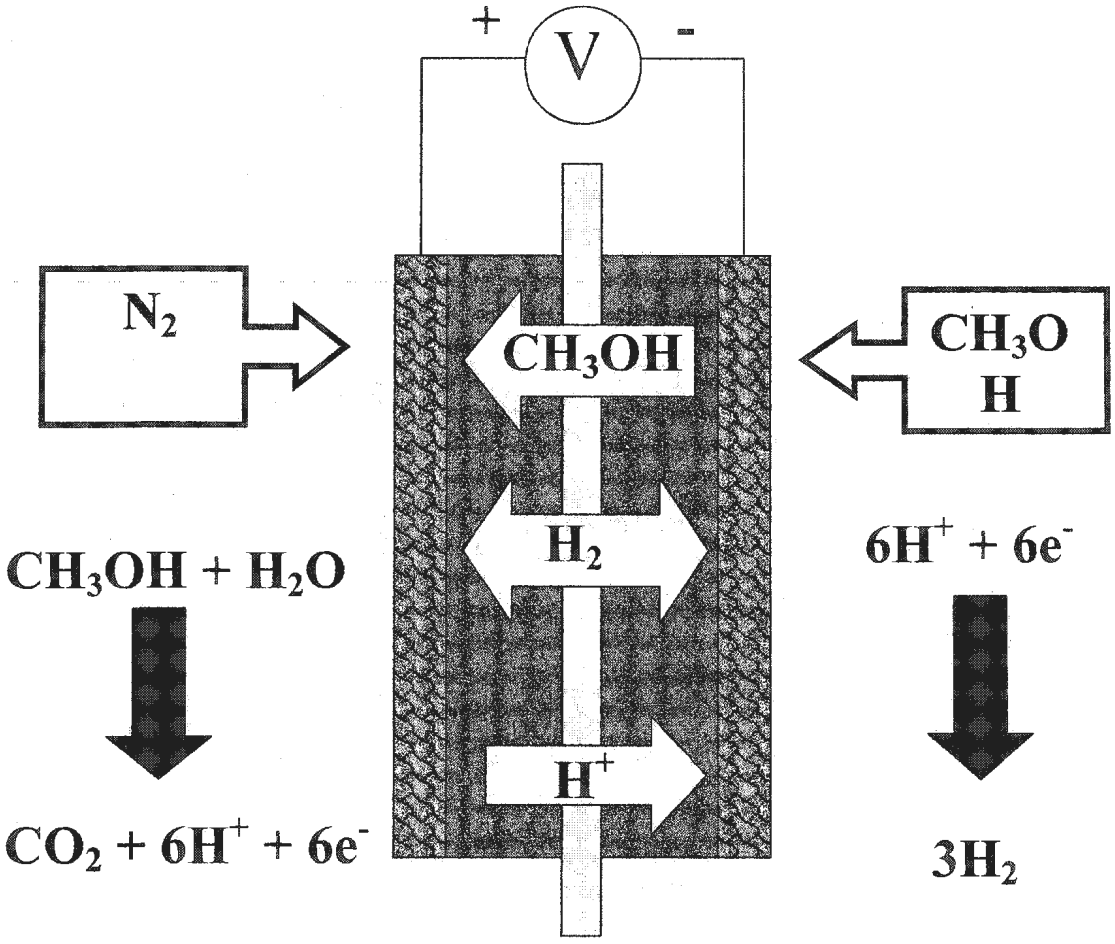

Figure 3.1. A schematic diagram showing the methanol permeation process and the electrode reactions involved in the electrochemical measurement of crossover.

Where C_m is the concentration of methanol within the membrane, D_m is the diffusion coefficient of methanol, K_{dl} is the drag coefficient, d is the membrane thickness, and F is the Faraday constant.

The methanol flux is retarded by the migration of protons in the opposite direction. Values of K_{dl} then, are less than unity, and decrease with increasing methanol concentration. Ren has calculated a K_{dl} value of 0.8829 for 1 mol L^{-1} methanol.[5]

Many factors affect methanol crossover in a DMFC. The operating temperature has a great influence on methanol transport, as increasing the temperature will increase the diffusion coefficient of methanol, and so more methanol crossover occurs.[10] Nafion® (membrane) thickness has also been shown to affect methanol crossover.[8] Increasing the thickness minimizes methanol crossover. However, this is accompanied by an increase in the ionic resistance of the membrane which, unfortunately, causes performance losses.[8]

Modification of Nafion® membranes has been utilized to minimize membrane permeation towards methanol. Several approaches have been reported,[11,12] and will be discussed in chapter 4.

The objectives of the work described in this chapter were to study and investigate the influences of operating temperature, membrane thickness, and molar concentration of methanol on methanol crossover. Here, methanol crossover measurements were made by electrochemical methods.

The first scheme was the investigation of methanol crossover dependence on temperature. The DMFC was run at different operating temperatures (30, 40, 50, and 60 °C). In general, increasing the temperature will cause an increase in the methanol crossover rate and affect the performance of the cell.

The second scheme was to study the membrane thickness affect on methanol transport. Four different thicknesses of Nafion® were investigated (112, 1135, 115, and 117) and their permeability to methanol was measured. This terminology contains the equivalent weight (EW) of Nafion® polymer used, and the thickness of the membrane. The first two integers represent the EW (definition in section 1.4.1.) of polymer, and the other numbers give the membrane thickness in milliinch. For example, Nafion® 1135 indicates that the EW of the polymer is 1100 grams per mole of sulfonate groups, and the thickness is 3.5 milliinch (~89 μm). The membrane thicknesses are therefore: 112 (~51 μm) <1135 (~89 μm) <115 (~127 μm) <117 (~178 μm). All membranes have an EW of 1100 g eq^{-1}.

The methanol feed (fuel) concentration influence on methanol permeability was investigated in the third scheme. Different molar concentrations of methanol (0.1, 0.3, 0.6, and 1.0 mol L^{-1}) were used in the DMFC. Generally, methanol crossover increases with higher concentration of methanol. On the other hand, using higher concentrations affects the performance of the cell. In order to explore these effects, cell polarizations (cell voltage vs current density) also were measured.

3.2 Experimental

3.2.1 Electrodes and Catalysts

Anodes and cathodes used in the experiments described in this chapter were supplied by Ballard Power Systems. Anodes consisted of a PTFE bound mixture of platinum black with a total Pt loading of 4.0 mg cm^{-2} and rhodium black with a total Rh loading of 1.3 mg cm^{-2} on carbon fiber paper (CFP, Toray T090) containing *ca.* 18% PTFE. Cathodes consisted of a PTFE bound mixture of platinum black with a total Pt loading of 4 mg cm^{-2} on CFP (Toray T090) containing *ca.* 11% PTFE.

Although these electrodes do not provide very good DMFC performance (cf. chapter 4), they are adequate for studies of methanol crossover. Better electrodes did not become available until later in the project.

3.2.2 Membrane Electrode Assembly (MEA) Preparation

Nafion® membranes were cleaned as described in section 2.3.1. MEAs were assembled according to the procedure described in section 2.3.2. However, the MEAs were first pressed at room temperature for 90 seconds under 1000 pounds force, followed then by hot pressing at 130 °C, under a force of 400 pounds.

3.2.3 Crossover and Polarization Measurements

Determination of methanol permeation rates through the membranes was accomplished by running methanol fuel through the anode, and an inert gas (N_2) was run through the cathode compartment (see figure 3.1 for equations). All the experiments were performed with a methanol pumping rate (f_{MeOH}) of 2.25 mL min^{-1} and at N_2 flow rate of 23.2 mL min^{-1}.

DMFC polarization curves were obtained by passing oxygen through the cathode at a flow rate of 6.5 mL min^{-1} and with a methanol pumping rate of 0.153 mL min^{-1}. Polarization readings were measured by applying a constant current from the potentiostat/galvanostat. Voltage readings were recorded after a stabilizing time of 3 minutes to achieve a stable value.

The temperature of the DMFC for all the experiments in this section was controlled manually with a STACO Inc. Variable Autotransformer (Model 3PN1010).

3.3 Results and Discussion

3.3.1 Electrochemical Measurement of Methanol Crossover

Initially, methanol crossover data were obtained by using staircase linear sweep voltammetry. This electrochemical method was used to determine the potential range over which the limiting current occurs. Moreover, it provides information about the half wave potential ($E_{1/2}$) value. Figure 3.2 shows

voltammograms for a cell with a Nafion® 112 membrane operated at 50 °C using 0.1, 0.3, 0.6, and 1.0 mol L^{-1} methanol solutions.

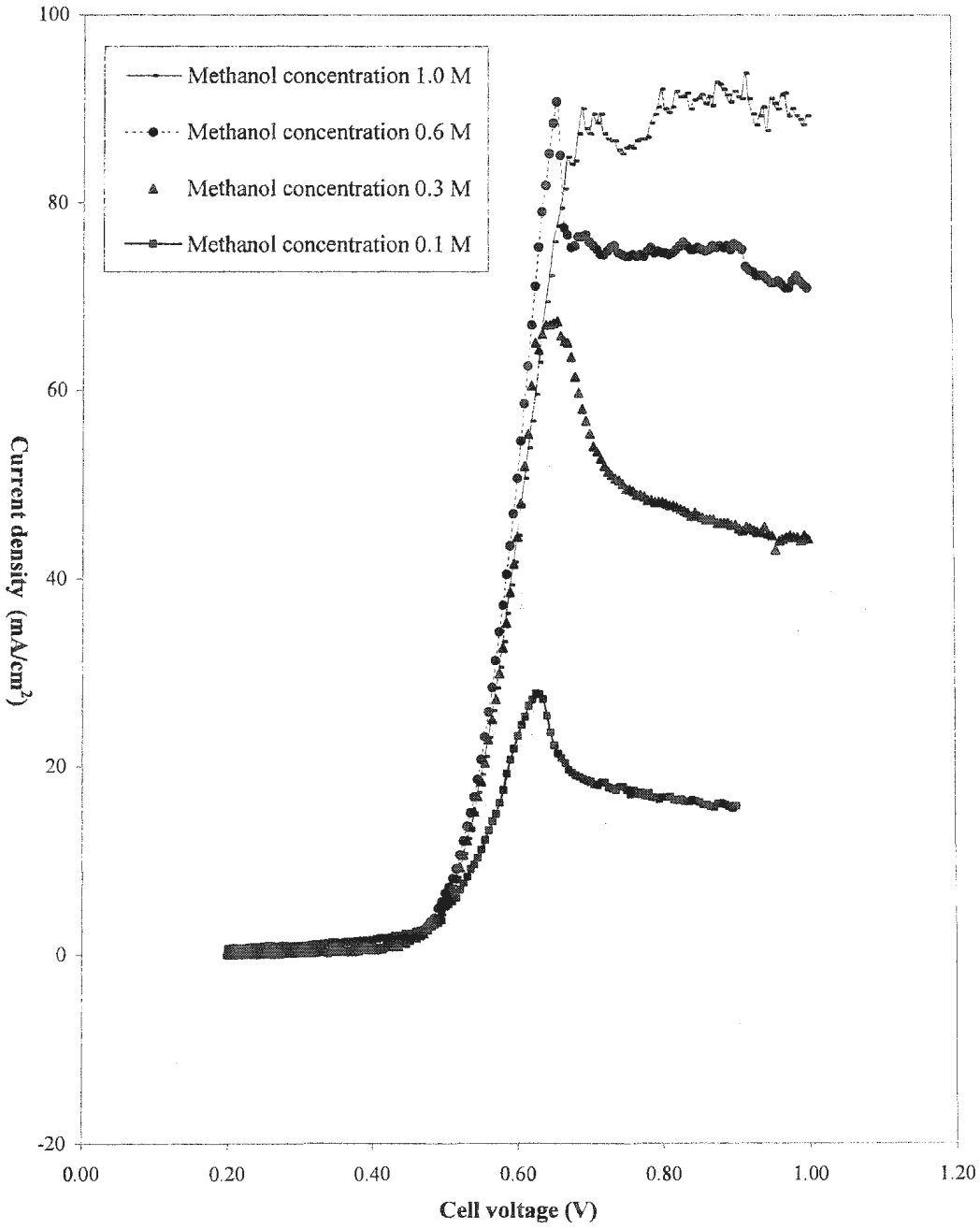

Figure 3.2. Voltammetric curves at 50 °C for the oxidation of methanol crossing through Nafion® 112 using 0.1, 0.3, 0.6, and 1.0 M methanol solutions, step height = 5 mV, step time = 2.5 s.

The current reaches its maximum value at *ca.* 0.6 V then drops to an approximately constant, limiting, value. The peak formation and the unsteady and decreasing limiting current values were major problems with this method. They result from the current not being allowed to reach its steady state value. The methanol concentration in the membrane is decreasing with time. To overcome these problems, the experiments may be performed at a lower scan speed to reach a steady state response but this was considered a too time consuming procedure.

A chronoamperometric method was used to overcome the scan rate dependency of the linear sweep method and therefore reduce the experiment time. The current in the new method is measured at steady state in a relatively short time. Moreover, it involves measuring the current at different programmed potential step values to ensure that the limiting current is obtained. Figure 3.3 shows a typical chronoamperometric potential time diagram.

The values of E1, E2, and E3 are initially set at 0.7, 0.8, and 0.7 V, respectively. The experiment is carried out and then these potential values may need to be increased or decreased slightly to achieve the limiting current plateau. The cell was conditioned for 50 second (t_1) at E1, to deplete the methanol in the membrane, and approach the limiting current. Then, the first methanol crossover measurement is started and extends for 100 second (t_2) at E2. The crossover measurement is repeated (at E3 for 100 second (t_3)) in the same experiment to insure that the data correspond within 5% and represent the limiting current.

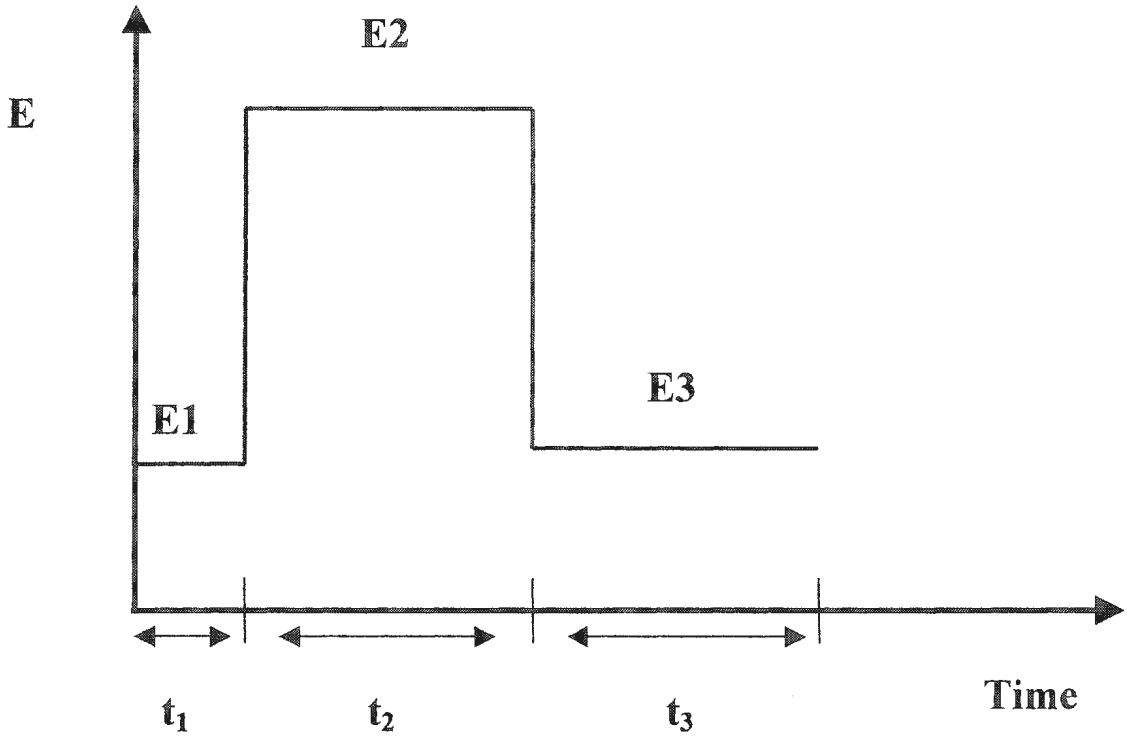

Figure 3.3. Chronoamperometric potential time diagram.

The limiting current values were calculated by averaging the current values for the last 40 seconds of the two potential step (E2 and E3) curves. Then, the values were divided by the area of the MEA and reported as current density values.

Table 3.1 summarizes the methanol crossover measurements collected by chronoamperometry for different Nafion® membranes, tested over a range of temperatures, and methanol concentrations. I_{lim} is proportional to the diffusion coefficient and concentration as per equation 3.1.

Table 3.1. Methanol crossover measurements for Nafion membranes.

		Methanol crossover (mA cm^{-2})			
Nafion® membrane	**Methanol Conc. (M)**	**@ 30 °C**	**@ 40 °C**	**@ 50 °C**	**@ 60 °C**
112	**0.1**	9.47	13.7	18.4	23.9
	0.3	25.5	36.2	47.6	59.5
	0.6	51.0	71.6	92.3	117
	1.0	85.3	118	153	192
1135	**0.1**	3.43	7.20	9.72	12.6
	0.3	17.5	23.8	31.0	40.2
	0.6	37.9	49.5	64.6	78.2
	1.0	60.5	80.5	105	129
115	**0.1**	3.46	5.40	7.77	11.0
	0.3	15.1	20.5	27.2	34.9
	0.6	31.6	42.5	55.8	69.7
	1.0	53.8	73.0	92.0	115
117	**0.1**	2.97	5.31	7.69	10.3
	0.3	13.6	18.1	24.1	30.5
	0.6	26.4	36.8	48.2	60.0
	1.0	47.6	63.5	80.6	99.2

3.3.2 Temperature Dependence (30, 40, 50, and 60 °C)

In order to investigate the temperature effect on methanol crossover, the same MEA was operated with different methanol concentrations at 30, 40, 50, and 60 °C. The relationship between the limiting current density and the temperature is controlled by Arrhenius equation:

$$I_{lim} = A\, e^{(-E_a/RT)} \qquad Eq.\ 3.2$$

Where A is a constant, E_a is the activation energy, R is the gas constant, and T is the temperature.

By taking the natural logarithm of Eq. 3.2, a linear relationship between $\ln(I_{lim})$ and $1/T$ is obtained, as follows:

$$ln(I_{lim}) = ln(A) - \frac{E_a}{R}\frac{1}{T} \qquad Eq.\ 3.3$$

Figure 3.4 illustrates the temperature dependence of methanol crossover for Nafion® 117. Obviously, increasing the temperature is coupled with an increase in methanol crossover towards the cathode compartment. Methanol crossover values were increased more than 200% as the temperature was raised from 30 to 60 °C for all the membranes. This phenomenon is also observed and verified for Nafion® 112, 1135, and 115.

Increasing the temperature causes an increase in the methanol diffusion coefficient within the membrane along with that of water molecules. Ren *et al.*,[5] have investigated the limiting current and diffusion coefficient of methanol over a range of temperatures. They reported the limiting currents for Nafion® 117 at 30

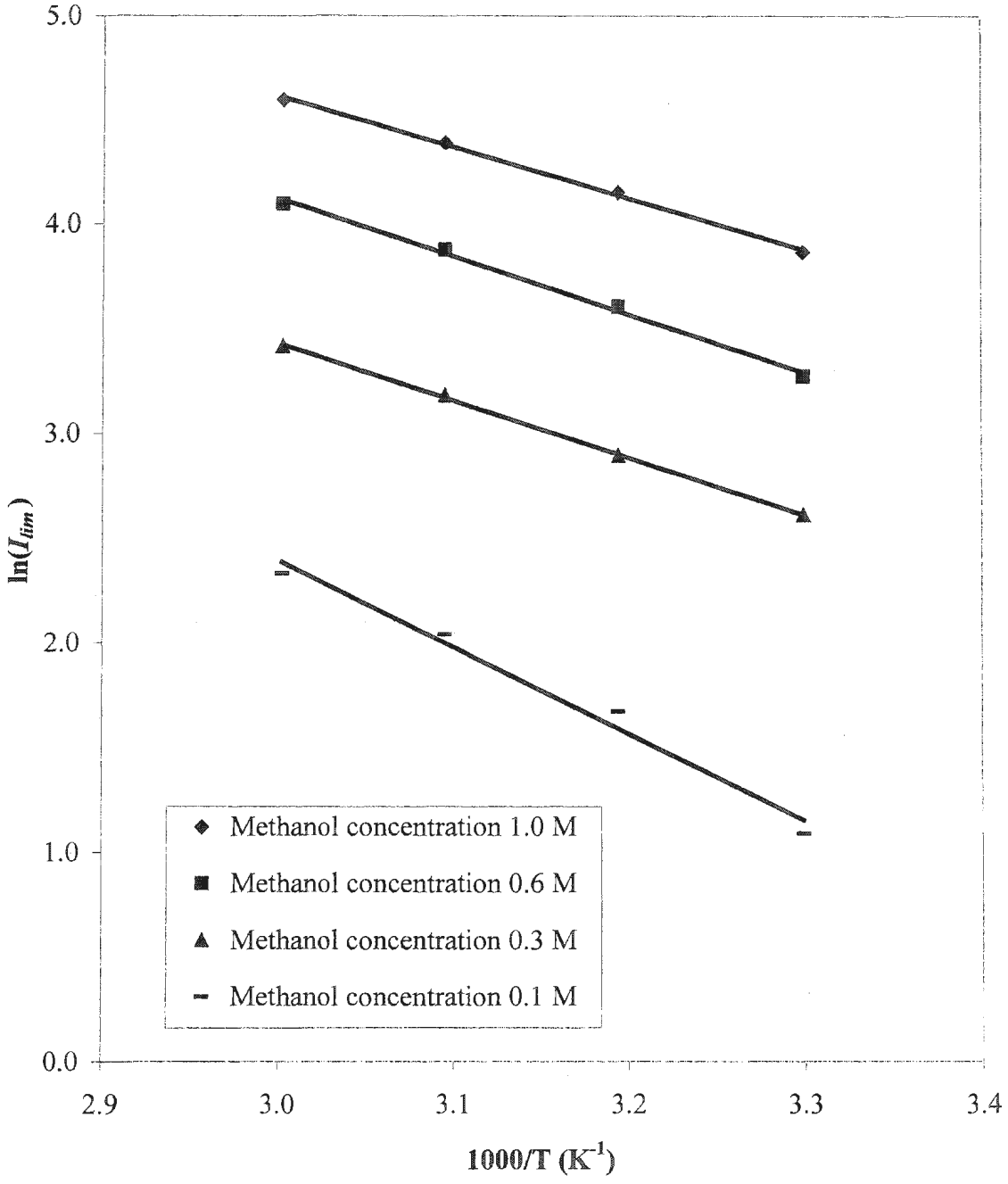

Figure 3.4. Temperature dependence of methanol crossover for Nafion®

117.

and 50 °C using 1.0 mol L^{-1} methanol solution as 42.0 and 76.6 mA cm^{-2}, respectively. The diffusion coefficient increased by almost 178 % as the temperature was increased from 30 to 50 °C. Their crossover values are close to the measurements reported here for Nafion® 117 under the same conditions.

Table 3.2 illustrates the activation energy values for the membranes calculated using *Eq.* 3.3. At 0.1 mol L^{-1} of methanol, the activation energy shows a maximum value, then it decreases with increasing concentration of methanol. This may be related to the hydration level of the membranes. However, it is not clear that the variations in table 3.2 are significant. The average value is 25 kJ mol^{-1}.

Table 3.2. Activation energies from *Eq.* 3.3.

		Activation Energy (kJ mol^{-1})			
	Methanol Conc. (M)	**0.1**	**0.3**	**0.6**	**1.0**
Nafion membrane	**112**	26	24	24	23
	1135	35	23	20	21
	115	32	24	22	21
	117	34	23	23	20

Several researchers have investigated the activation energy for methanol diffusion in Nafion. Ren and co-workers have reported values of 20[5] and 24[13] kJ

mol^{-1} which are similar to the values reported here. However, it seems to be affected by the experimental condition and environment.[14]

Despite the fact that methanol crossover causes performance losses and reduces the open circuit potential (OCP), increasing the temperature increases proton mobility in Nafion®.[15] Therefore, operating the DMFC at a higher temperature increases the proton conductivity of the MEA, resulting in a better performance of the fuel cell as shown previously in figure 1.4.

3.3.3 Thickness Dependence (Nafion® 112, 1135, 115, and 117)

Since the MEA can be considered as a physical barrier that separates the anode from the cathode, the current density (I_{lim}) is controlled and affected by the membrane thickness. The relationship between I_{lim} and membrane thickness is given by equation 3.1.

However, the limiting current density is also influenced by the anode (including the backing and the catalyst layers), which behaves as an additional diffusion barrier ($I_{lim,anode}$). Therefore:

$$\frac{1}{I_{lim}} = \frac{1}{I_{lim,anode}} + \frac{1}{K_{dl}} \frac{d}{nFC_mD_m} \qquad Eq.\ 3.4$$

Figure 3.5 shows a plot of the reciprocal of the limiting current density (I_{lim}^{-1})(from *Eq.* 3.4) versus thickness for a set of membranes at 30, 40, 50, and 60 °C, using 1 mol L^{-1} methanol solution. The results do not fit the expected linear relationship closely. The deviation could be due to a number of factors such as,

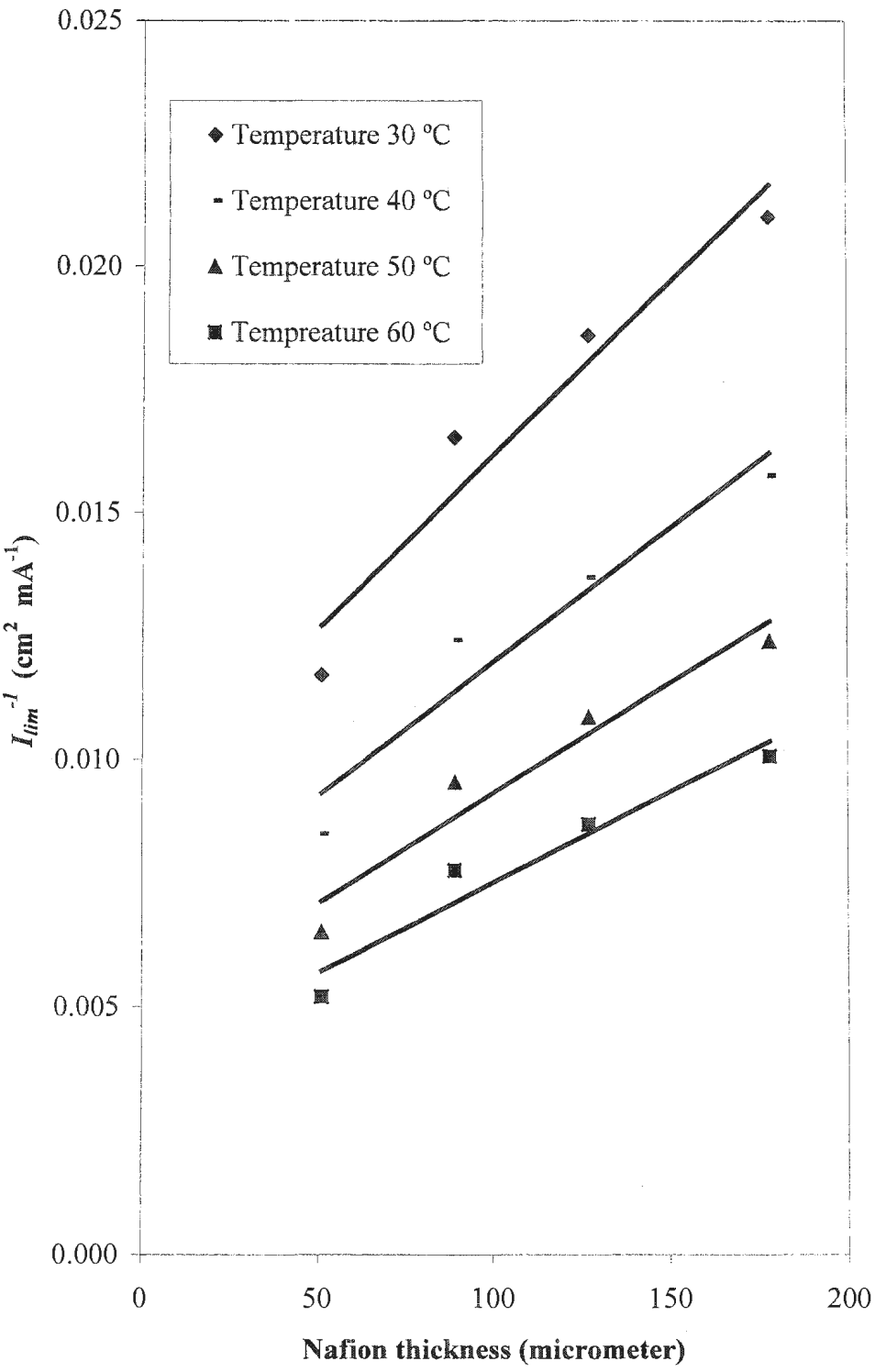

Figure 3.5. Thickness dependence of methanol crossover for a series of membranes using 1 mol L^{-1} methanol solution at different temperatures.

variation in the electrode and the membrane characteristics.

As expected, methanol crossover decreases with increasing membrane thickness. These results confirm that the methanol pumping rate was sufficient to overcome the high permeability of the thinner membranes. For a fuel cell of 5 cm^2, I_{lim} has been reported to become independent of methanol flow rate at methanol feeds of more than 0.75 mL min^{-1}.[5]

Ren and co-worker[5] have reported that $I_{lim,anode}$ has no significant effect on the methanol crossover measurements. Therefore, the anode shows a high permeability to methanol and does not affect the anode performance. Table 3.3 illustrates the $I_{lim,anode}$ values obtained from the intercept of figure 3.5. The result shows that anode permeability is not that high and it does affect the methanol crossover. For example, if there were no anode ($I_{lim,anode}$ goes to zero), the I_{lim} value for Nafion® 117 membrane at 60 °C would be 140 mA cm^{-2} (instead of 99.2 mA cm^{-2}), which is *ca.* 41% more. This may be related to the anode structure as Ren[5] used a thin carbon cloth backing, while carbon paper is the backing for the anode used in the experiments reported here.

Table 3.3. $I_{lim,anode}$ values obtained from figure 3.5.

Temperature (°C)	$I_{lim,anode}$	Standard Deviation
30	110	19
40	152	30
50	204	42
60	256	56

3.3.4 Concentration Dependence (Methanol Concentration 0.1, 0.3, 0.6, and 1.0 mol L^{-1})

The influence of methanol concentration on methanol transport had been investigated for different Nafion® membrane thickness at the same temperature. The I_{lim} was measured, and then plotted as a function of methanol concentration. Increasing the methanol feed concentration to the DMFC is expected to increase methanol crossover through the membrane and therefore reduce the overall performance and lower the fuel efficiency.

Figure 3.6 shows methanol crossover measurements for a series of Nafion® membranes at 60 °C using different concentrations of methanol. Methanol crossover increased at least 8 times for Nafion® membranes as the methanol concentration was increased from 0.1 to 1 mol L^{-1}.

As a matter of fact, the methanol crossover of a DMFC operated with low methanol feed concentrations (less than 2 mol L^{-1}) is decreased at high current densities,[13] and fortunately, the DMFC performance is improved. This may be explained by the fact that most of the methanol is consumed by oxidation at the anode before it can cross through the membrane to the cathode.

Figure 3.7 shows polarization curves of a DMFC operated at 60 °C with 1 mol L^{-1} methanol feed, using a Nafion® 115 membrane. At current densities up to *ca.* 20 mA cm^{-2}, the performance of the cell is decreased as the methanol concentration is increased. Moreover, the OCP decreased from 742 to 521 mV as the methanol concentration was increased from 0.1 to 1 mol L^{-1}.

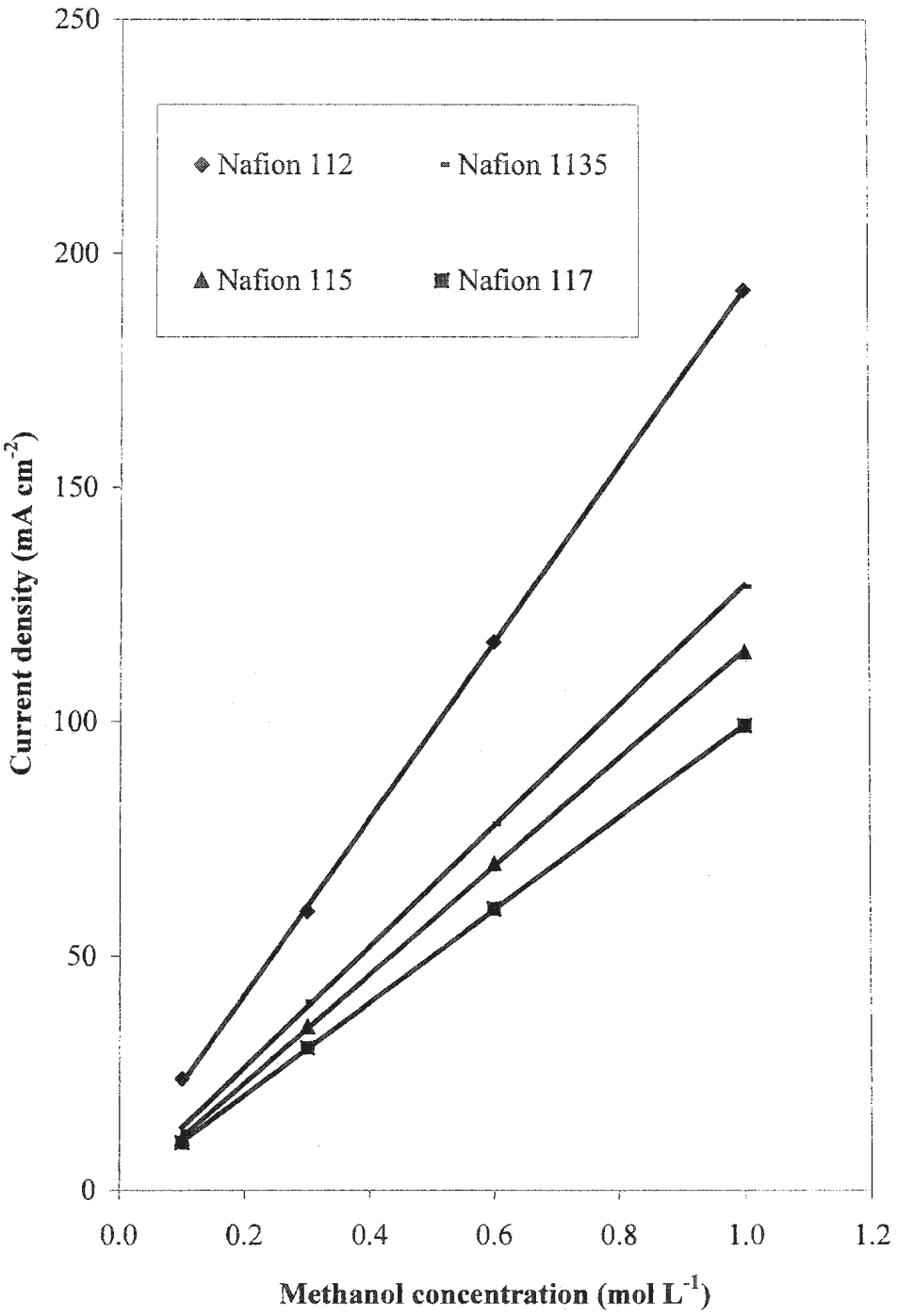

Figure 3.6. Concentration dependency of methanol crossover for a series of Nafion® membranes at 60 °C.

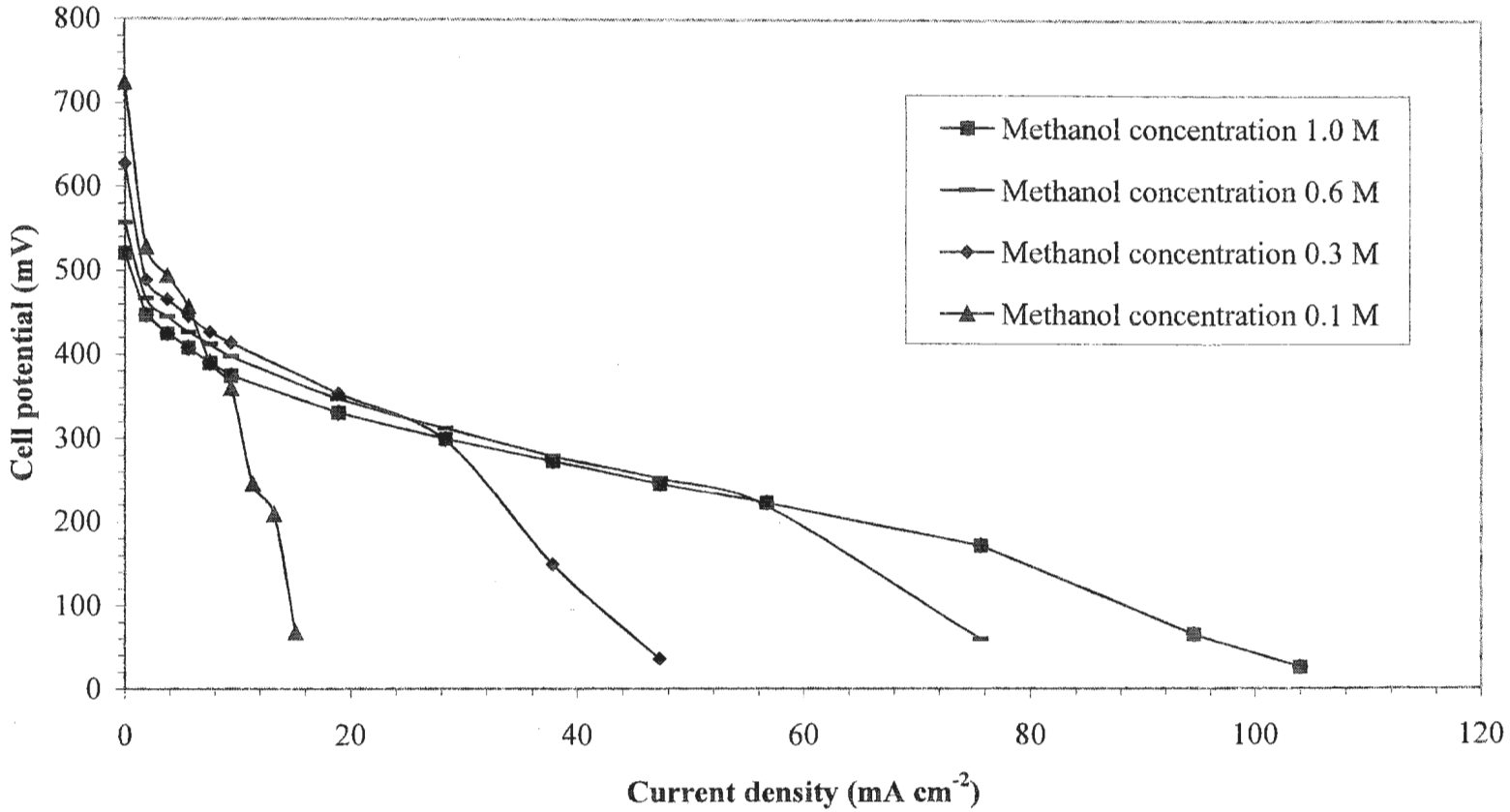

Figure 3.7. Polarization curves of a DMFC operated at 60 °C using a Nafion® 115 membrane with different methanol concentrations.

On the other hand, at high current densities, the performance of the DMFC was significantly improved by increasing the methanol concentration and the fuel cell provide best performance operating with 1 mol L^{-1} methanol solution.

3.4 Conclusions

Methanol crossover in a DMFC was measured directly by double-step chronoamperometry. This method minimizes the time required for the measurements and provides verified measurements of the steady state crossover current.

Methanol crossover was measured over a set of different temperatures. The results show a significant increase of methanol permeation through the membrane with increasing temperature. Moreover, an Arrhenius type relationship was observed. The activation energy of methanol diffusion was calculated and shows a value of 25 kJ mol^{-1} (average value of 16 measurements). Ren and co-workers have reported values of 20[5] and 24[13] kJ mol^{-1} which are similar to the values here.

The experimental results emphasized that methanol permeation is decreased as the thickness of membrane is increased. The crossover value decreased by more than 50% (at 60 °C and 1 mol L^{-1} methanol) as the thickness was increased from 51 (Nafion® 112) to 178 (Nafion®117) μm. This improves the fuel efficiency of the cell, however, increasing the membrane thickness is

accompanied by an increase in resistance,[10] which therefore leads to Ohmic losses and poor performance.

Although methanol crossover increases linearly with concentration, the performance of the cell substantially improves at high current densities. The best DMFC performance was obtain using 1 mol L^{-1} methanol, although, 0.6 mol L^{-1} also shows a good performance.

Several parameters affect methanol diffusion through the membrane, and therefore influence the overall performance of the DMFC. Methanol crossover in DMFCs operated with Nafion® membranes is still undesirable and causes high energy and fuel losses. Modification of Nafion® membranes could probably reduce the crossover and improve the cathode activity. Also, the optimal operating conditions for DMFCs are still under investigation to improve DMFC performance.

References

[1] Hobson, L. J.; Ozu, H.; Yamaguchi, M.; Hayase, S.; *J. Electrochem. Soc.* **2001**, 148, 10, A1185-A1190.

[2] Shao, Z.-G.; Hsing, I-M.; *Electrochem. Solid-State Lett.* **2002**, 5, 9, A185-A187.

[3] Carrette, L.; Friedrich, K. A.; Stimming, U.; *ChemPhysChem* **2000**, 1, 162-193.

[4] Lamy, C.; Léger, J-M.; Srinivasan, S.; *Modern Aspects of Electrochemistry*, No. 34, Bockris, J. O'M; Conway, B. E., Eds; Kluwer Academic/Plenum Publishers: New York, **2001**, pp 53-118.

[5] Ren, X.; Springer, T. E.; Zawodzinski, T. A.; Gottesfeld, S.; *J. Electrochem. Soc.* **2000**, 147, 2, 466-474.

[6] Ren, X.; Springer, T. E.; Gottesfeld, S.; *J. Electrochem. Soc.* **2000**, 147, 1, 92-98.

[7] Thomas, S. C.; Ren, X.; Gottesfeld, S.; Zelenay, P.; *Electrochim. Acta* **2002**, 47, 3741-3748.

[8] Arico, A. S.; Srinivasan, S.; Antonucci, V.; *Fuel Cells*, **2001**, 1, No. 2, 133-161.

[9] Walker, M.; Baumgartner, K.-M.; Kaiser, M.; Kerres, J.; Ullrich, A.; Rauchle, E.; *J. Appl. Polym. Sci.* **1999**, Vol. 74, 67-73.

[10] Heinzel, A.; Barragan, V. M.; *J. Power Sources*, **1999**, 84, 70-74.

[11] Uchida, H.; Mizuno, Y.; Watanabe, M.; *J. Electrochem. Soc.* **2002**, 149, 6, A682-A687.

[12] Jia, N., Lefebvre, M. C.; Halfyard, J.; Qi, Z.; Pickup, P.G.; *Electrochem. Solid-State Lett.* **2000**, 3, 12, 529-531.

[13] Ren, X.; Zawodzinski Jr., T. A.; Uribe, F.; Dai, H.; Gottesfeld, S.; *Electrochemical Society Proceedings*, Vol. 95-23.

[14] Kauranen, P. S., Skou, E.; *J. Appl. Electrochem.* **1996**, 26, 909-917.

[15] Buchi, F.; Scherer, G. G.; *J. Electrochem. Soc.* **2001**, 148, 3, A183-A188.

Chapter 4

Characterization of DMFC Performance and Methanol Crossover through Modified Membranes

4.1 Introduction

Modification of Nafion® membranes has been utilized to minimize membrane permeation towards methanol. For example, silicon oxide,[1] zirconium phosphate[2] and conducting polymers[3] have been incorporated into Nafion® membranes, to produce composite membranes with better properties, and therefore, a better overall DMFC performance.

Composite membranes show less permeability to methanol and therefore methanol crossover is decreased and fuel efficiency is improved. Composite membranes prepared by using poly(1-methylpyrrole) reduce methanol crossover by as much as 50% without a significant increase in membrane resistance.[4]

This chapter characterizes the performance of DMFCs operated with polypyrrole/Nafion composite membranes. Methanol crossover through these membranes is also investigated, and the results are compared with results obtained for unmodified Nafion® membranes. Composite membranes prepared using 3,4 ethylene-dioxythiophene (EDOT) were also studied to some extent but require further investigation.

4.2 Experimental

4.2.1 Electrodes, Catalysts and MEA Preparation

Anodes and cathodes used in the experiments described in this chapter were prepared by Brad Easton.[5] Anodes consisted of a Nafion (15%) bonded mixture of 50% Pt and Ru black with a total loading of *ca.* 4 mg cm^{-2} on CFP

(Toray T090) containing 10% Nafion. Cathodes consisted of a PTFE bound mixture of Pt black with a total loading of *ca.* 4 mg cm^{-2} on CFP (Toray T090) containing 15% PTFE, and were sprayed with Nafion solution to give a 14% loading.

Nafion® membranes were cleaned as described in section 2.3.1. MEAs were assembled according to the procedure described in section 2.3.2.

4.2.2 Crossover and Polarization Measurements

Determination of methanol permeation rates through modified and unmodified membranes was accomplished as described in section 3.3.1. However, the experiments were performed with a N_2 flow rate of 25.6 mL min^{-1}.

DMFC polarizations were obtained by passing either oxygen (12.3 mL min^{-1}) or air (73.1 mL min^{-1}) through the cathode compartment, and with a methanol pumping rate of 0.153 mL min^{-1}. Polarization readings were measured as described in section 2.4.

4.2.3 Resistance Measurements

The resistance of the fuel cell was measured by Electrochemical Impedance Spectroscopy (EIS). The measurements were made while passing either oxygen, air or nitrogen through the cathode compartment and methanol through the anode. The results were not significantly influenced by the cathode gas (for example, the resistance of unmodified Nafion 115 with N_2 and O_2 was

0.169 and 0.159 Ω, respectively). Unless stated otherwise, the final resistance measurement is reported.

4.2.4 Preparation of Polypyrrole/Nafion Composite Membranes

Polypyrrole/Nafion membranes were prepared by *in situ* polymerization of pyrrole within Nafion membranes in the presence of H_2O_2 or Fe^{3+} as an oxidizing agent.

Some composite membranes prepared using H_2O_2 as the oxidizing agent were synthesized by Brandi Langsdorf and are coded as BLXXXX. On the other hand, Jeremy Hughes synthesized one of the composite membranes using Fe^{3+} as the oxidizing agent and it is therefore coded as JHXXXX. Several membranes were synthesized by myself using either H_2O_2 or Fe^{3+} as the oxidizing agent and are therefore coded as XJ (e.g. 4J).

The procedure of preparation of the composite membranes (prepared by the author), using either of the oxidizing agents, involves immersing a clean piece of Nafion membrane of the desired size in a pyrrole solution of certain concentration for a certain amount of time (minutes or hours). Following brief washing with water, the pyrrole impregnated membrane is immersed in a solution containing the oxidizing agent for several minutes or hours to achieve polymerization.

All the composite membranes were washed with hot 1 mol L^{-1} H_2SO_4 solution several times until the acid remained colorless, in order to wash out any residual pyrrole and oxidizing agent in the membrane. The last step was to soak

the composite membrane in hot water for at least 1 hour to remove the excess acid. Finally, the composite membranes were stored in water at room temperature.

4.2.5 Preparation of Poly(EDOT)/Nafion Composite Membranes

A cleaned piece of Nafion was immersed in neat EDOT for 30 minutes, then washed with water and transferred to the oxidizing solution (Fe^{3+}) for 30 minutes. Another membrane was immersed in 0.1 M EDOT solution (50% acetonitrile/H_2O) for 15 minutes, then washed with water and transferred to 5% H_2O_2 solution for 5 min to achieve polymerization. The membranes were then washed and stored as in section 4.2.4.

4.3 Results and Discussion

4.3.1 Oxygen vs Air Cathode Feed

Initially, DMFC performance was investigated by running pure O_2 through the cathode compartment. O_2 produces better DMFC performance than air and the performance differences between membranes can be more easily observed. However, running a DMFC using air is preferable from a commercial point of view as it reduces the operating cost, simplifies the system and is safer.

DMFC performances for modified and unmodified Nafion 115 with O_2 or air on the cathode are compared in figure 4.1. For unmodified Nafion 115, there was a 14% voltage loss at *ca.* 56 mA cm^{-2} as the DMFC oxidant gas was switched to air; moreover, it decreased by 22% at *ca.* 94 mA cm^{-2}.

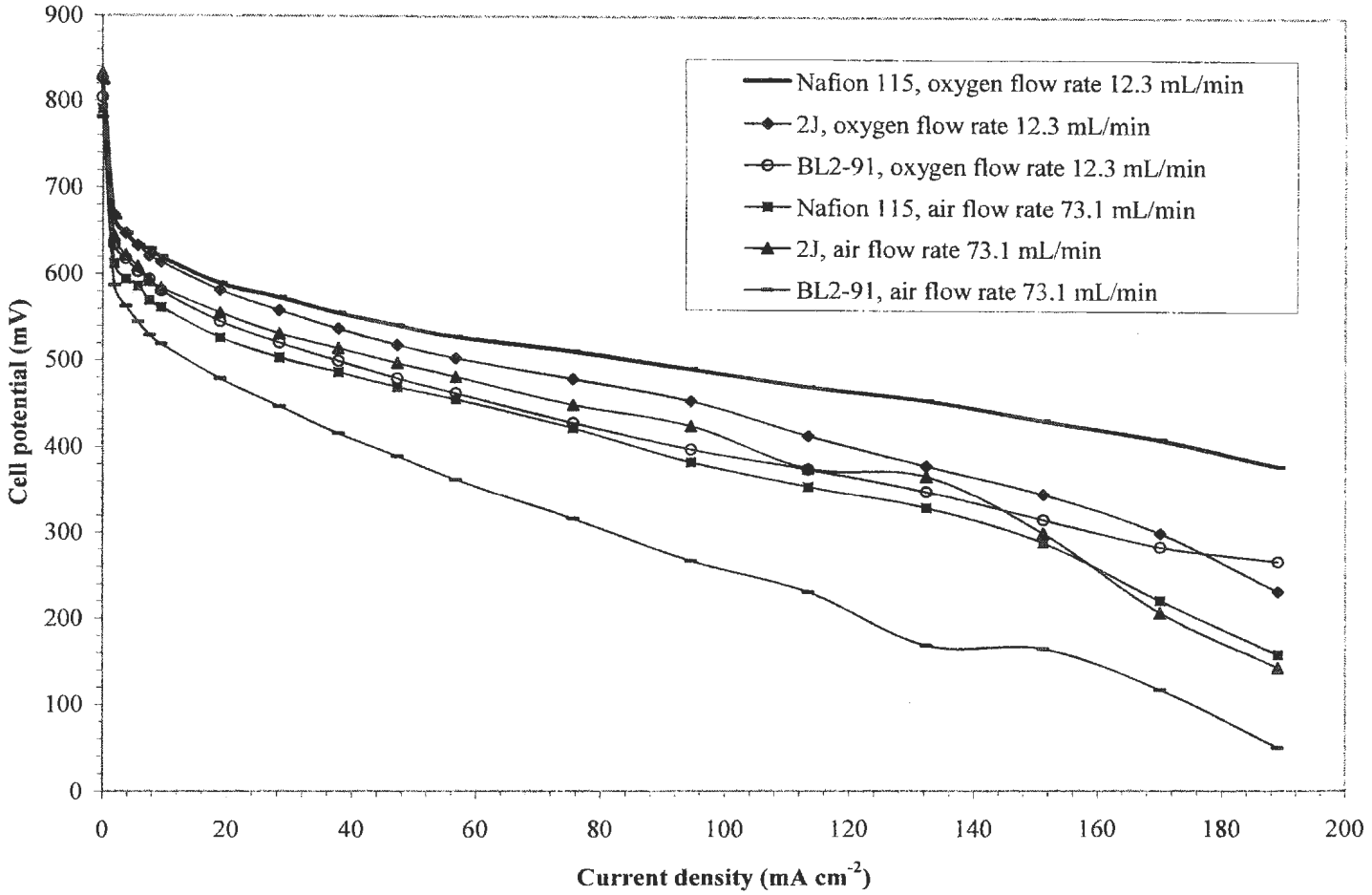

Figure 4.1. DMFC performances for unmodified and modified Nafion 115 running with oxygen or air at 60 °C and at ambient pressure. C_{MeOH} = 1 mol L^{-1}.

The BL2-91 composite membrane losses were greater (22% and 33% lower), while the performance with 2J decreased by only 4% and 6%, at the same current densities.

These comparisons were performed at ambient pressure and a lower performance was always obtained when air was employed. This could be related to the difference in oxygen concentration in the cathode chamber. The test for Nafion and BL2-91 membranes was performed using air four months after it was tested with oxygen, however, for 2J the DMFC was tested with air after one day. This may explain the poor performance of these membranes with air.

Running a DMFC with pure oxygen gas provides more oxidant species at the cathode side. The better DMFC performance running with O_2 could be expected from thermodynamics (Nernest equation), as increasing the concentration of O_2 in the cathode feed gas leads to an increase in the theoretical cell voltage. Moreover, this improves and speeds up oxygen mass transport to catalyst active sites, and therefore drives the cathodic reaction to reduce more oxygen. Advantageously, more oxygen improves the oxidation of CO_{ads} (formed at the catalyst surface as a result of methanol oxidation at the cathode) to CO_2, therefore decreasing the CO poisoning effect at the cathode, and therefore optimizes the overall cell performance.

On the other hand, air provides an excess of gas to flush water from the cathode compartment. Moreover, a high airflow rate enhances the oxidation of methanol and reduces the effect of methanol crossover on the cathode catalyst.[6]

As well, increasing the gas pressure leads to better performance as the methanol crossover rate is decreased.[7]

4.3.2 Performance of Polypyrrole/Nafion Composite Membranes Prepared by H_2O_2 Oxidation

Modification of Nafion 115 membranes with polypyrrole using H_2O_2 as the oxidizing agent shows good blockage of methanol. The composite membranes reduce methanol crossover by ca. 42-74%. However, the resistance of these membranes was variable and dependent on the modification procedure. Table 4.1 summarizes the characteristics of the membranes tested in this work.

Table 4.1. Modification conditions, methanol crossover and resistance measurements for unmodified and modified Nafion 115.

Membrane	Time in 0.2 M pyrrole (min)	Time in 30% H_2O_2 (min)	I_{lim} @ 60 °C* (mA cm^{-2})	R* (Ω cm^2)
Nafion 115	-	-	136	0.16
1J	15	15	35.7	0.89
2J	5	5	78.4	0.29
BL2-91	5	5	70.3	0.34

* Represent average values except for 1J.

DMFC performances for these composite membranes are illustrated in figure 4.2. Although, 1J, a modified Nafion 115 membrane, exhibits the best methanol blockage, it shows poor DMFC performance. This membrane was immersed in both the pyrrole and the oxidizing agent solution for a longer time than the other membranes, therefore more polypyrrole is present in the membrane which results a higher resistance than the other modified membranes.

2J exhibits good DMFC performance. At low current densities (< 20 mA cm^{-2}), it shows a similar performance to unmodified Nafion 115. The similar performance in this region may be related to the improvement of cathodic reactivity as a result of lower methanol crossover. On the other hand, the performance decreased with increasing current density. For example at *ca.* 100 mA cm^{-2}, 2J only produced 455 mV compared to 492 mV for Nafion 115. The increased membrane resistance is responsible for these performance losses. From Ohm's law, a calculated 0.13 Ω cm^2 difference in membrane resistance decreases the cell voltage by 13 mV at *ca.* 100 mA cm^{-2}. Therefore, a resistance corrected potential value of 468 mV is obtained, which may be considered to be within experimental error of the value for Nafion 115.

Figure 4.3 reveals the cell performances running with air. 2J shows an excellent performance. This membrane was the best membrane tested and outperforms Nafion 115 by *ca.* 11% at *ca.* 100 mA cm^{-2}. However, the performance of BL2-91 was lower by about 4%, at the same current density.

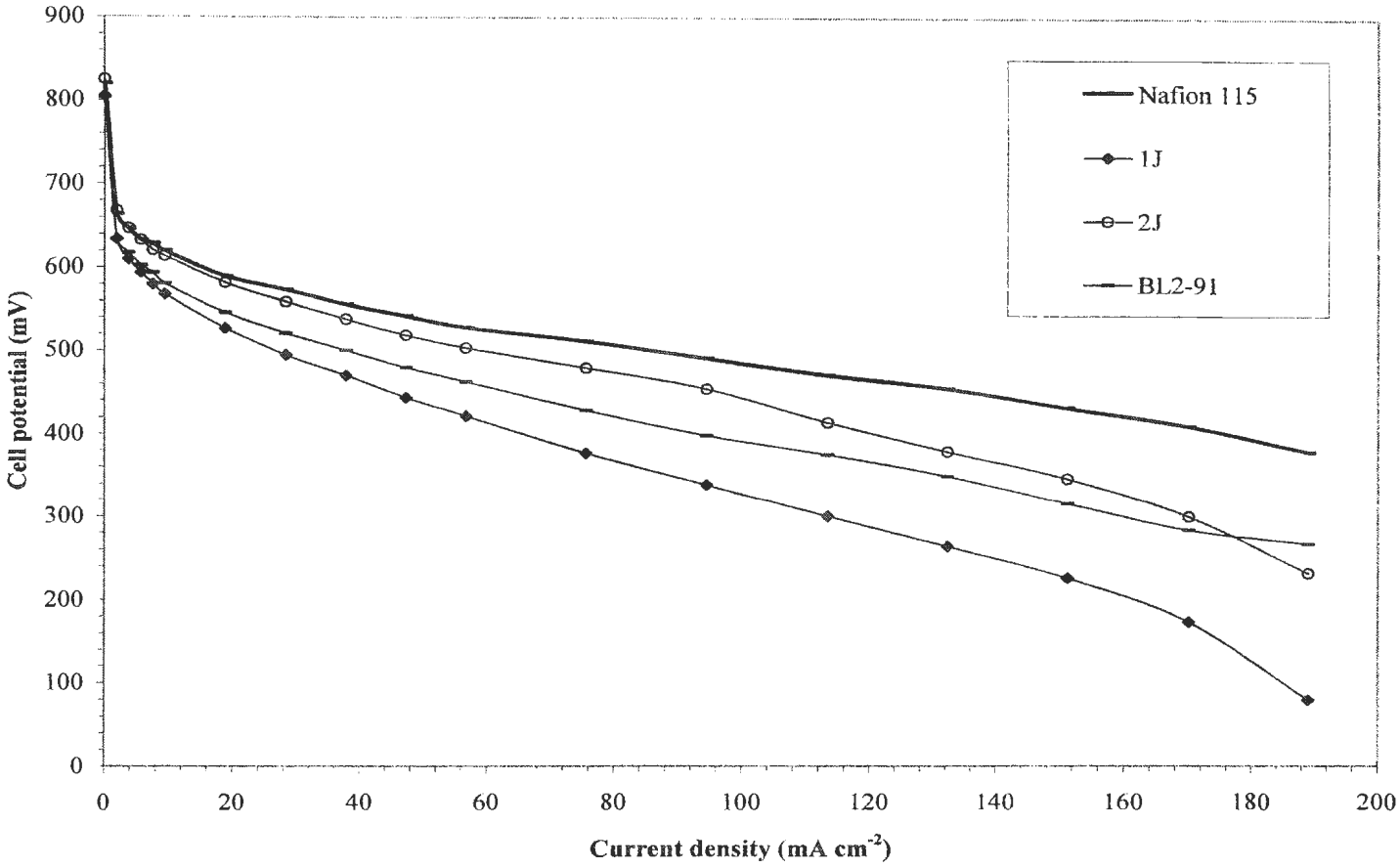

Figure 4.2. DMFC performances for unmodified and modified Nafion 115 membranes running with oxygen at 60 °C and at ambient pressure. f_{oxygen} = 12.3 mL min^{-1}, C_{MeOH} = 1 mol L^{-1}.

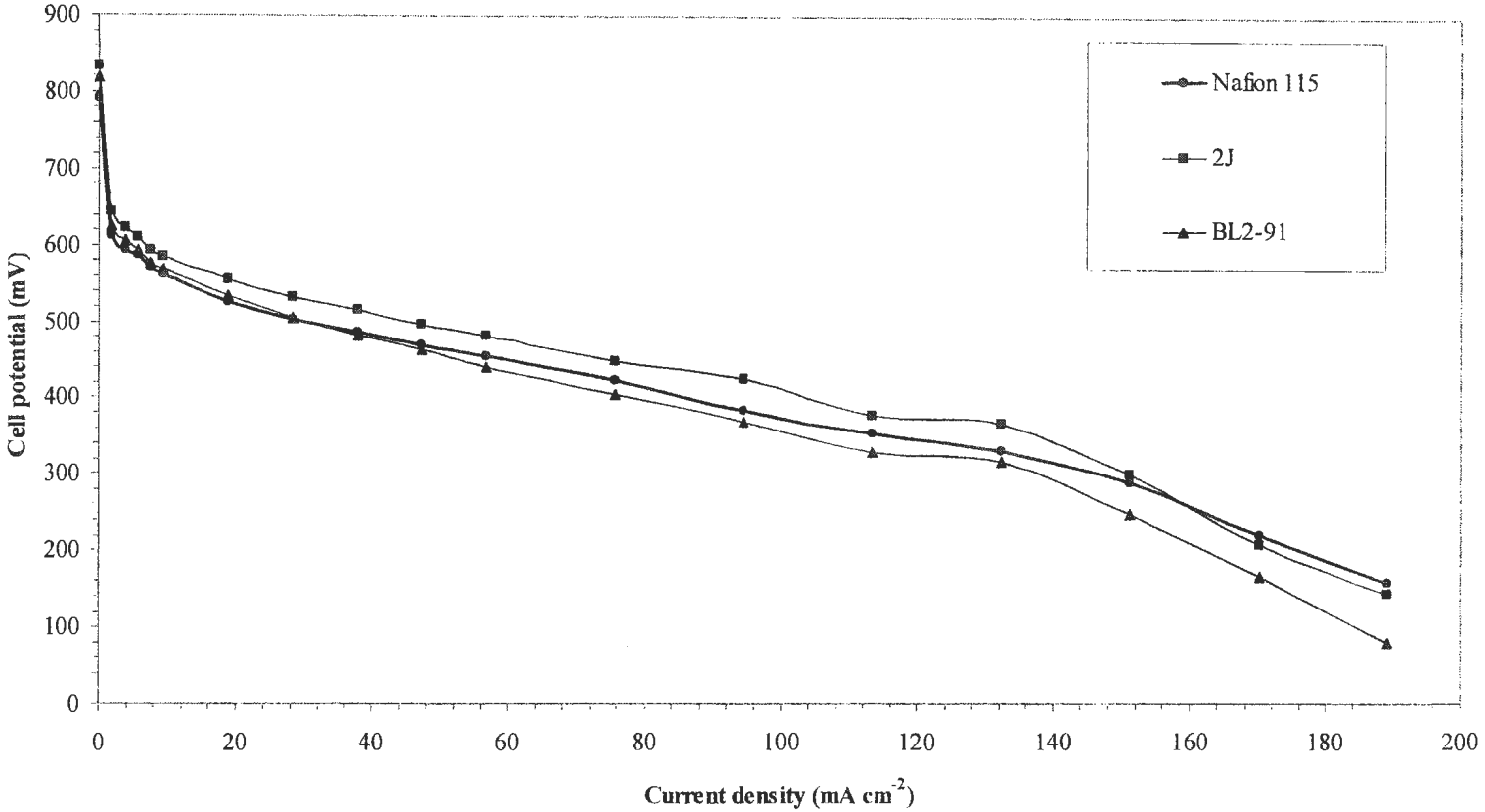

Figure 4.3. DMFC performances for unmodified and modified Nafion 115 membranes running with air at 60 °C and at ambient pressure. f_{air} = 73.1 mL min^{-1}, C_{MeOH} = 1 mol L^{-1}.

Running DMFC with air rather than O_2, increases the effect of methanol crossover on the cathode. The effect of the decreased crossover through the modified membranes is therefore more pronounced with air.

4.3.3 Performance of a Polypyrrole/Nafion Composite Membrane Prepared by Fe^{3+} Oxidation

Several membranes were modified by Jeremy Hughes using the Fe^{3+} oxidation method. However, data for only one will be presented here. Earlier membranes investigated employed inferior electrodes (as described in section 3.2.1) with low catalytic activity which produced poor cell performance. Furthermore, the modified membranes did not appear to bond well to these electrodes. Therefore, their data will not be discussed in this thesis.

Composite membrane JH1028b shows an excellent performance and a low resistance value of 0.23 Ω cm^2. Although, its methanol crossover was high (114 mA cm^{-2}), this membrane was the 2^{nd} best membrane tested and outperformed Nafion 115 by 7% at *ca.* 100 mA cm^{-2} as shown in figure 4.4.

As expected from the membrane resistance, Ohmic voltage losses are small relative to the unmodified membrane as revealed by the resistance corrected curve. However, there is still a window for further modification to further reduce methanol crossover, as this membrane decreased it by just 16% (compared to Nafion 115).

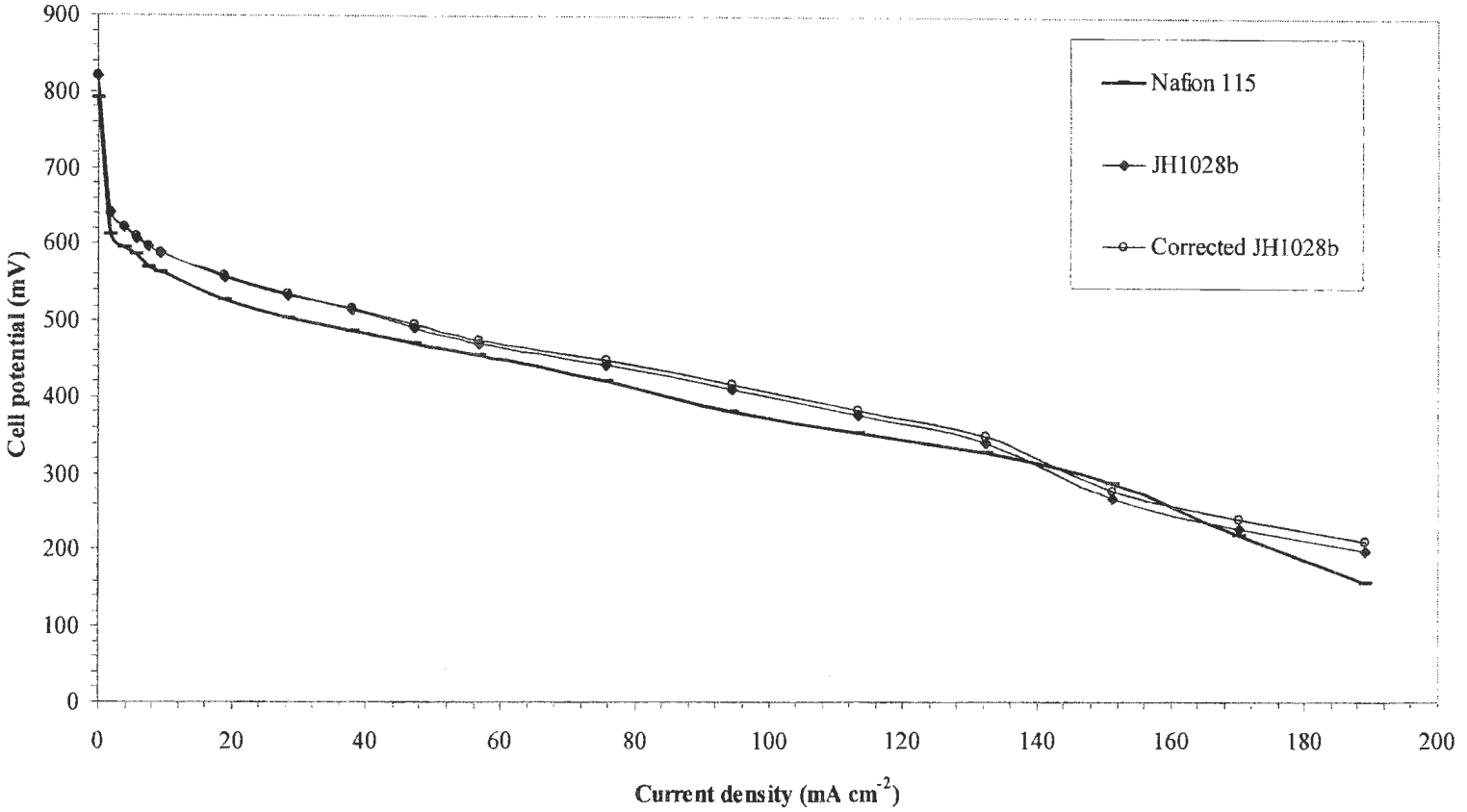

Figure 4.4. DMFC performances of Nafion 115 and JH1028b membranes running with air at 60 °C and at ambient pressure, f_{air} = 73.1 mL min^{-1}, C_{MeOH} = 1 mol L^{-1}. The corrected JH1028b data has been adjusted to the same cell resistance as unmodified Nafion 115 (0.16 Ω cm^2).

4.3.4 Effect of Modification Method on Composite Membrane Performance

H_2O_2 modification produces composite membranes with high methanol blockage but with variable resistance values which often lead to Ohmic voltage losses and reduced cell performance. On the other hand, Fe^{3+} modification formed a composite membrane with low resistance but with only 16% methanol blockage. Thus a combination of both treatments was employed to try to gain the benefits of each and, hopefully, fabricate a composite membrane with reasonable methanol blockage without increasing the membrane resistance significantly.

Nafion membranes were modified by *in situ* polymerization of pyrrole using H_2O_2 as the oxidizing agent followed by further polymerization via Fe^{3+} oxidation. The performances of 6 composite membranes with different modification procedures were investigated. The Nafion 115 membranes were first immersed in 0.2 mol L^{-1} pyrrole solution for 5 min, and then immersed in 30% H_2O_2 for 5 min. Then 5 of them were immersed in $Fe(NO_3)_3$ solution for further polymerization for different time periods. Table 4.2 summarizes the characteristics of these composite membranes.

The performances of the composite membranes improved greatly with time. The first run for each MEA in the DMFC gave a poor performance; however, an improved and stable performance was achieved after 3 days. A stability test of one composite membrane for two weeks over a set of temperatures

shows a peak performance after 3 days (compared to less than 1 day for unmodified membranes).[5]

Table 4.2. Characteristics of polypyrrole/Nafion 115 composite membranes, prepared with H_2O_2 and Fe^{3+}.

Membrane	**Time in 0.08 M Fe^{3+} (min)**	**I_{lim} @ 60 °C* (mA cm^{-2})**	**R* (Ω cm^2)**
Nafion 115	-	136**	0.16**
8J	0	60.1	0.66
9J	1	45.0	1.3
10J	2	54.2	0.92
11J	3	48.2	0.88
12J	4	48.5	0.80
13J	5	54.2	0.85

* Represents the last measurement obtained.
** Represents an average value.

Figure 4.5 demonstrates the performance of 8J over a 3 days period. The performance improved with time and reached a steady value after 3 days. This appears to be related to the hydration level of the membrane during the test which affects its proton conductivity.[8,9] In the first run the MEA is dry as a result of hot pressing during its preparation. With operation, the membrane gains water slowly and its conductivity increases accordingly. For example, the resistance of 11J decreased by 95% over 3 days of operation (17, 1.1 and 0.88 Ω).

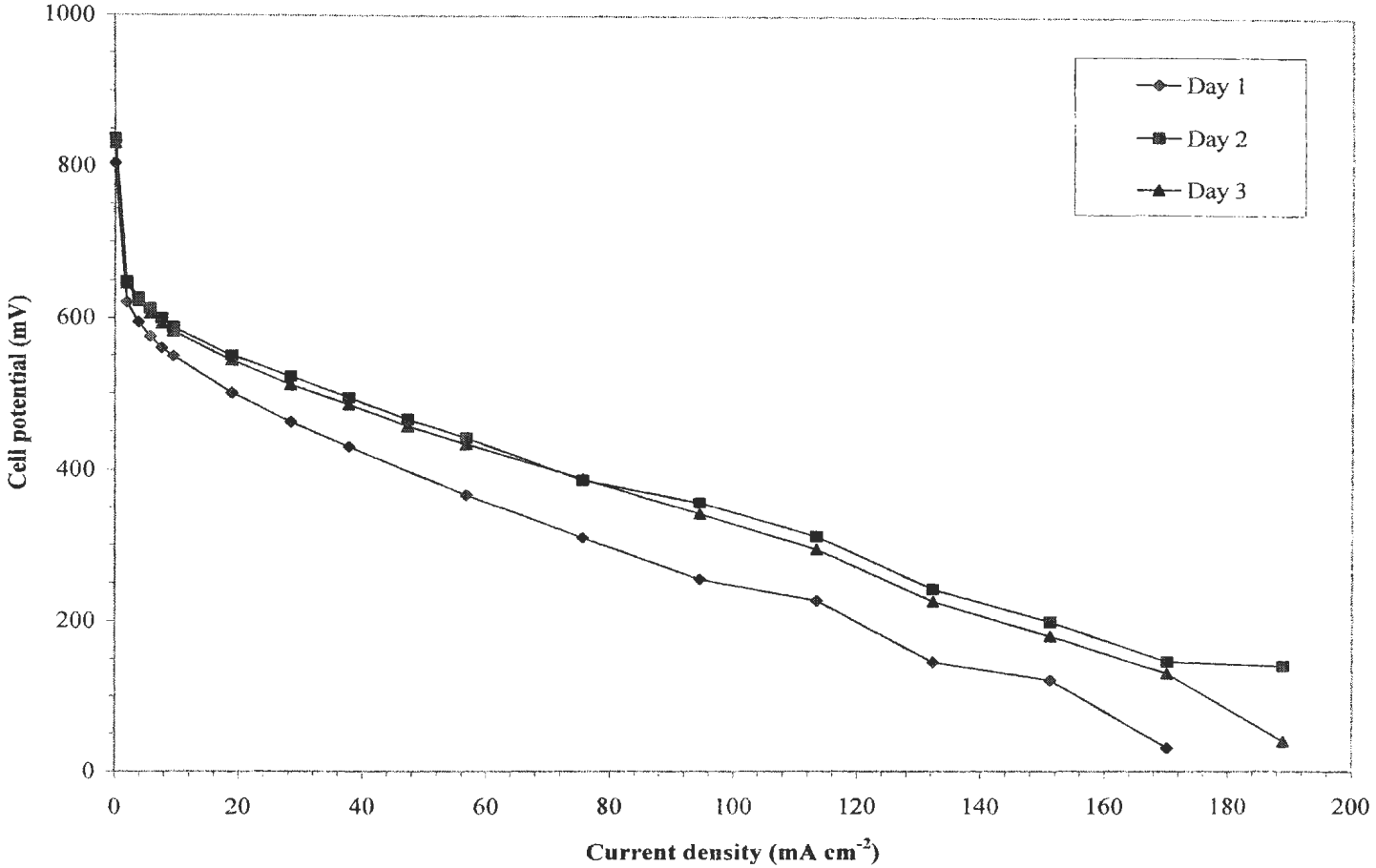

Figure 4.5. DMFC performance of 8J composite membrane running for 3 days with air at 60 °C and at ambient pressure. f_{air} = 73.1 mL min^{-1}, C_{MeOH} = 1 mol L^{-1}.

In table 4.2, further polymerization of polypyrrole/Nafion composite membranes with Fe^{3+} is seen to decrease methanol crossover by a further *ca.* 17% relative to one treated with H_2O_2 only. This is a result of more polypyrrole formation inside the membrane. Performance was expected to improve with this further reduction of methanol crossover, however, the DMFC showed worse performance as shown in figure 4.6.

Surprisingly, the performance was very poor for all the membranes that had been further treated with Fe^{3+}. Although 9J was immersed in the Fe^{3+} solution for the least time (1 min), it gave the worse performance. The performance, then improved as the immersion time was increased and reached its maximum performance with 11J and 12J.

Despite the reduction of methanol crossover for these membranes, their resistances were much higher than unmodified Nafion 115 which may be responsible for the poor DMFC performance. Although the resistance of 8J is higher than that of Nafion, it outperforms Nafion at low current densities (up to *ca.* 40 mA cm^{-2}). In figure 4.7, the cell potentials have been corrected to the resistance of Nafion 115 to investigate the resistance effect on DMFC performance. The resistance corrected performance is better. For example, it is improved, at *ca.* 100 mA cm^{-2} by 14, 27 and 24 % for 8J, 11J and 12J membranes, respectively.

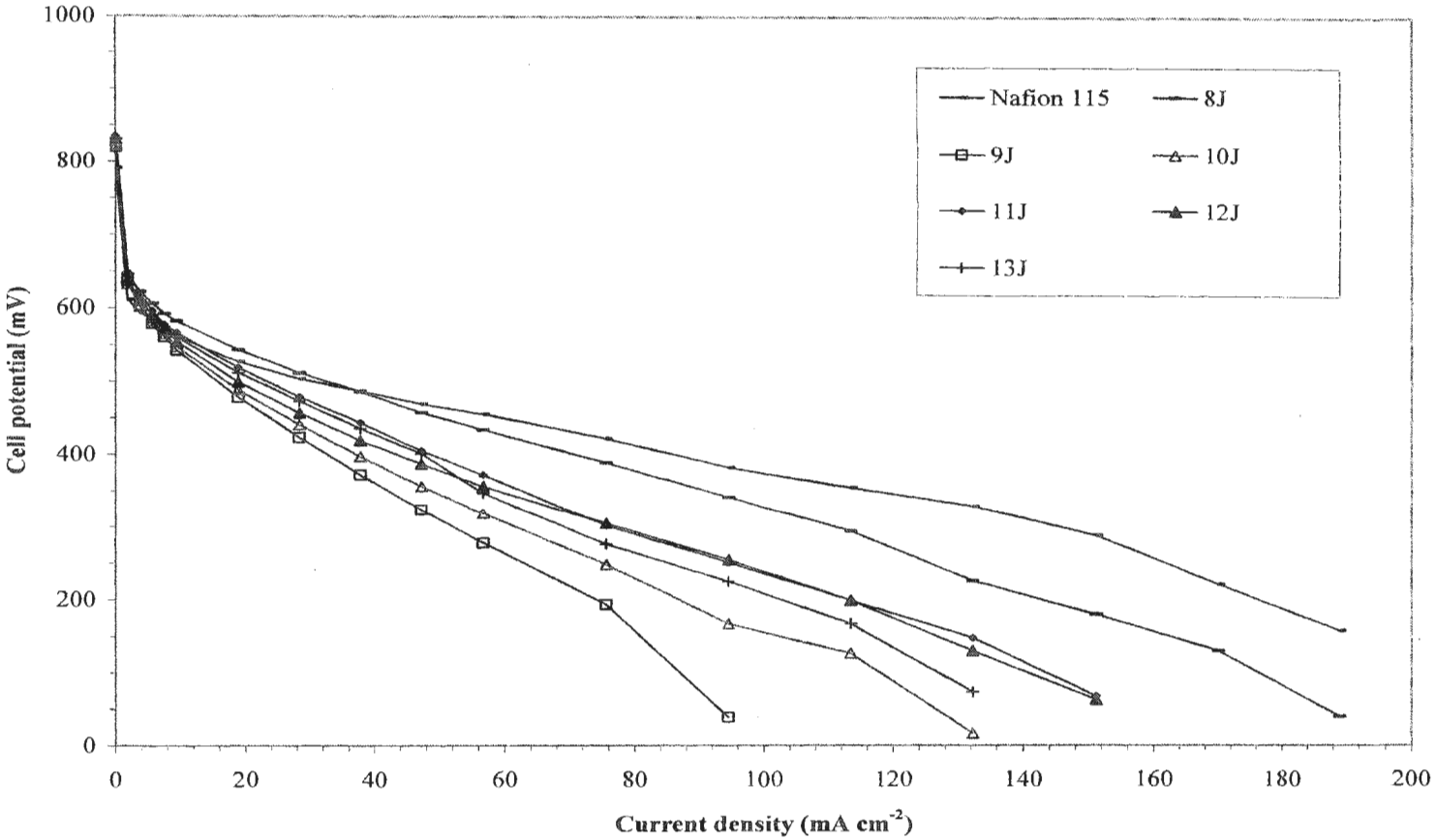

Figure 4.6. DMFC performances after running the cell for 3 days, for unmodified and modified Nafion 115 running with air at 60 °C and at ambient pressure. f_{air} = 73.1 mL min^{-1}, C_{MeOH} = 1 mol L^{-1}.

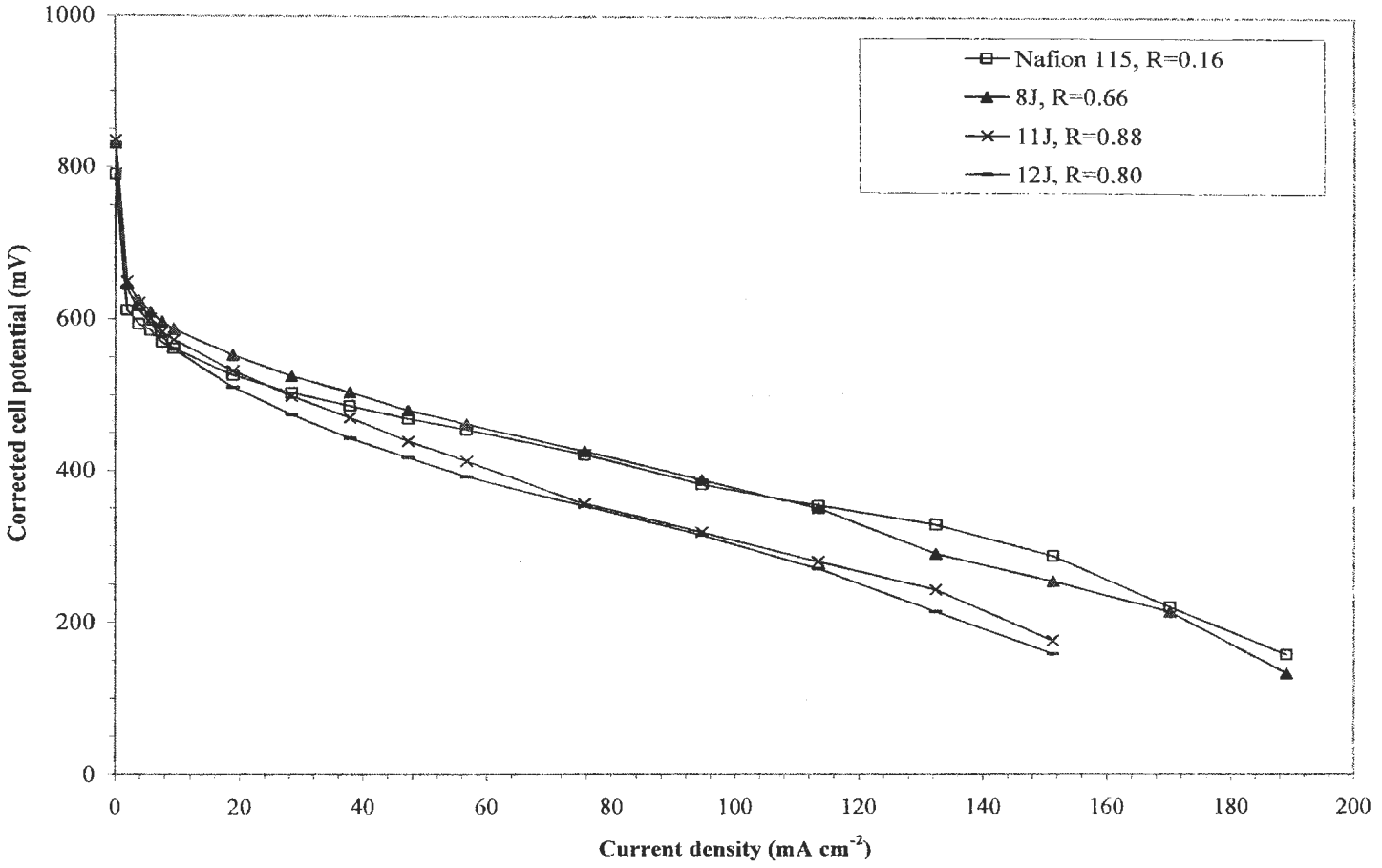

Figure 4.7. Resistance corrected DMFC performances for 8J, 11J and 12J membranes.

The corrected performance of 8J is almost the same as that of Nafion 115 which indicates that Ohmic losses are responsible for the poor performance in the high current density region. On the other hand, the corrected cell potentials of 11J and 12J are still far away from the expectation based upon Ohmic losses.

These composite membranes (treated with Fe^{3+}) show poor bonding to the electrodes, and delamination was observed. Sata *et al.*,[10] reported that polypyrrole is formed at the surface of the membrane in the presence of Fe^{3+} ions. This decreases the Nafion character at the surface of the membrane which therefore inhibits its bonding to the electrodes and reduces catalyst utilization at both electrodes and also increases resistance. Poor interfacial bonding properties for the membranes treated with Fe^{3+} severely reduce performance, and overcome the gains from methanol crossover minimization.

4.3.5 Modification of Nonacidic Nafion Membranes

Pickup et *al.*,[3] have reported that pyrrole undergoes a spontaneous reaction within Nafion membranes. The pyrrole monomer is protonated by the acidic nature of the ionic clusters and this leads to the formation of oligomeric and polymeric material during immersion of Nafion in the pyrrole solution.

The influence of membrane acidity on self polymerization can be minimized by cationic exchange of Nafion's protons, such that pyrrole uptake is controlled by diffusion and not by reactions within the membrane. A nonacidic form of Nafion115 (14J) was prepared by soaking the membrane in 1 mol L^{-1}

NaOH solution for *ca.* 14 hours. Then, both acidic Nafion (15J) and 14J were heavily modified by *in situ* polymerization of pyrrole via Fe^{3+} oxidation, followed by a washing procedure as in section 4.2.4. Table 4.3 summarizes the immersion times and results.

Table 4.3. 14J and 15J membrane characteristics.

Membrane	**Time in 0.2 M Pyrrole (hr)**	**Time in 0.08 M Fe^{3+} (hrs)**	**I_{lim} @ 60 °C* (mA cm^{-2})**	**R* (Ω cm^2)**
14J	1	10	119	0.22
15J	1	10	37.6	1.8
Nafion 115	-	-	136**	0.16**

* Represents the last measurement obtained.
** Represents an average value.

Even though both membranes were treated in the same way, they exhibit quite difference properties. Methanol crossover was decreased by ca. 12% and 72% for 14J and 15J, respectively, and they have quite different resistances. The performances of these membranes are shown in figure 4.8.

Although modified 15J gives the best open circuit voltage (821 mV, compared to 791 and 775 mV for Nafion 115 and modified 14J, respectively), it is clear that its performance is strongly affected by its high resistance, which is responsible for a performance loss of *ca.* 45% at *ca.* 100 mA cm^{-2} as shown from the resistance corrected potential curve. On the other hand, the performance of the

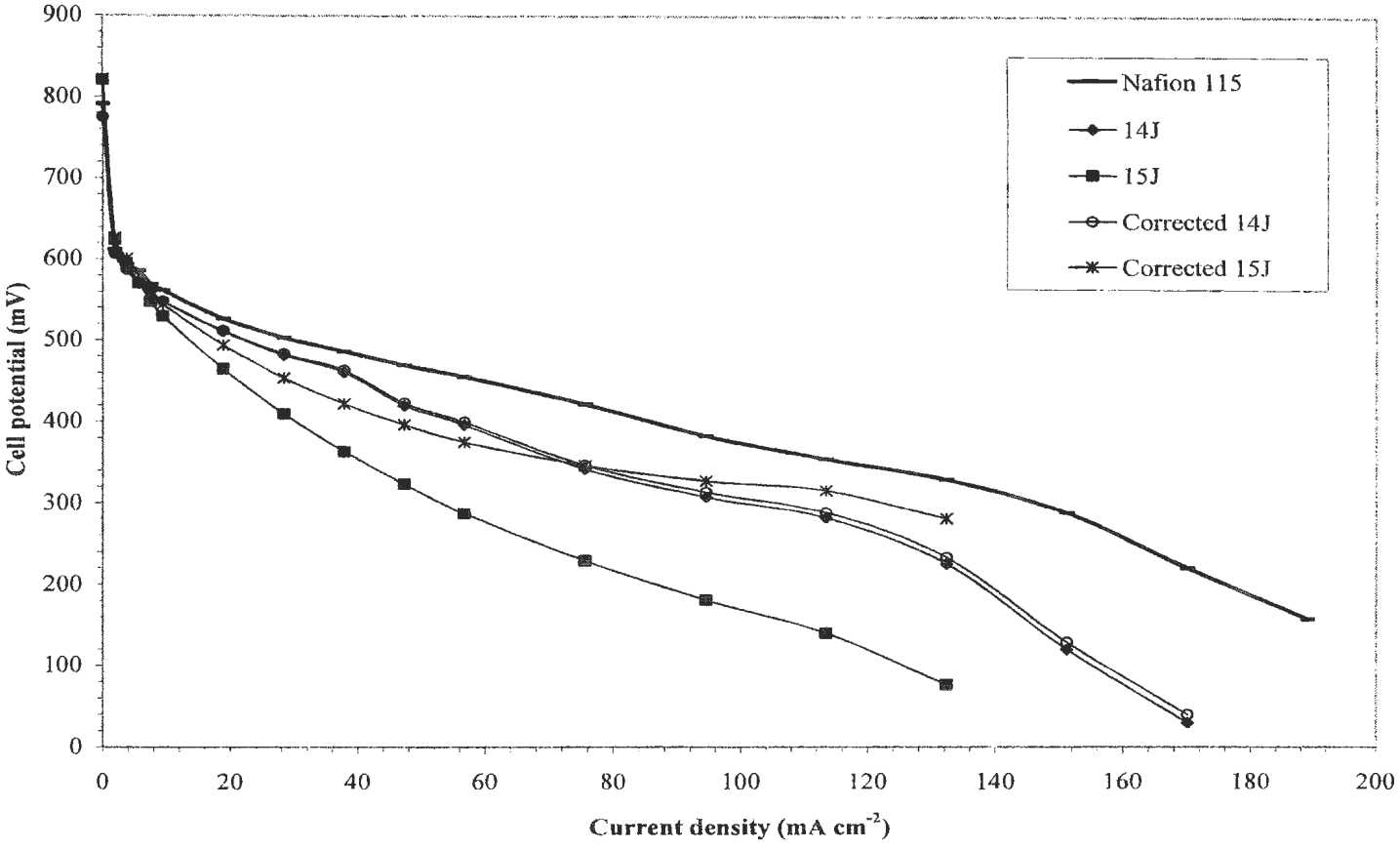

Figure 4.8. DMFC polarization curves for Nafion 115, 14J and 15J running with air at 60 °C and at ambient pressure. f_{air} = 73.1 mL min^{-1}, C_{MeOH} = 1 mol L^{-1}.

modified 14J membrane is *ca.* 20% less than that of Nafion 115 at *ca.* 100 mA cm^{-2}. This is difficult to understand since the resistance is close to unmodified Nafion 115 and so its performance losses are not Ohmic, as revealed from the corrected potential curve.

The poor performance could be explained by the difference in membrane acidity during the modification process. It is assumed that all of the H^+ were substituted by Na^+ in the 14J (Na-Nafion) and that 1 hour is enough time for pyrrole to fill the membrane pores. Therefore, pyrrole diffuses into 14J and fills the pores without reaction, while pyrrole in 15J (H-Nafion) spontaneously reacts with H^+ in the Nafion pores to form polymeric material. The polymerization step with Fe^{3+} causes the formation of a tight layer of polypyrrole at the surface of the membrane[11] which may prevent further growth of the polymeric layer inside the membrane.

It can be concluded that the 15J membrane will have more polymer inside the membrane than 14J, and that most of the pyrrole inside 14J remains unreacted, and will leach out during the acid wash step. Moreover, the poor performance of modified 14J could be related to poor bonding of the membrane with the electrodes which leads to higher resistance and therefore poor performance (see chapter 5).

The performance of 14J composite membrane reveals the possibility for further modification. Other composite membranes were prepared using higher

pyrrole concentrations and longer treatment times. Table 4.4 summarizes the characteristics of these membranes.

Table 4.4. Na-form Nafion Composite membrane characteristics.

Membrane	**Pyrrole Conc. (M) (dipping time 2 hrs)**	I_{lim} **@ 60 °C*** **(mA cm^{-2})**	**R*** **(Ω cm^2)**
16J	0.5	101	0.40
17J	1.0	18.8	6.0
18J	2.0	1.87	280
19J	5.0	1.98	25

-All the membranes were treated with 0.08 M Fe^{3+} solution for 10 hrs followed by acid wash as described in section 4.2.4.
*Represents the last measurement obtained.

DMFC performances of these membranes are shown in figure 4.9. Although the resistance of 16J was doubled relative to 14J, its performance is better by 18% at *ca.* 100 mA cm^{-2}. Moreover, methanol crossover was reduced by another 15%, and its performance is only slightly inferior to unmodified Nafion 115.

Further increases in pyrrole concentration show a steep reduction in methanol crossover and reaches its limit with 2 mol L^{-1} pyrrole concentration. However, a very poor performance was obtained for 17J115, while 18J and 19J produced no current in the DMFC. It can be seen from figure 4.9 that the poor performance of 17J is only partially caused by its higher resistance. Poor

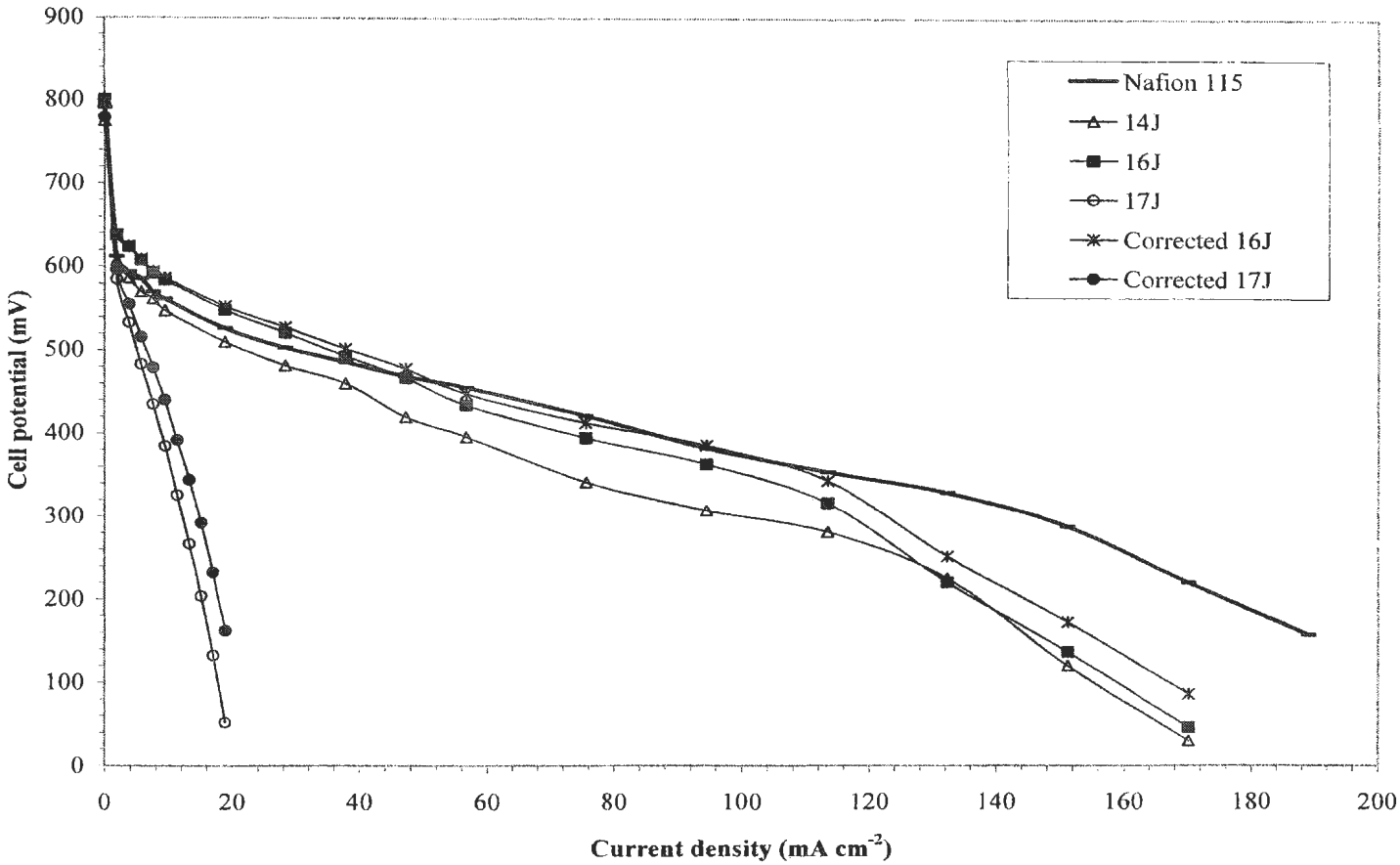

Figure 4.9. DMFC polarization curves for Nafion 115 and composite membranes running with air at 60 °C and at ambient pressure. f_{air} = 73.1 mL min^{-1}, C_{MeOH} = 1 mol L^{-1}.

interfacial bonding for this membrane causes delamination of the catalyst layers which severely reduces the performance.

These results suggest that the optimum modification of Nafion should produce a high level of polymeric material inside the membrane and high Nafion to polypyrrole character at the surface of the membrane. This would lead to good blocking of methanol and improve the electrode's cohesion with the composite membrane.

4.3.6 Performance of Poly(EDOT)/Nafion Composite Membranes Prepared by H_2O_2 and Fe^{3+} Oxidations

Since heavy modification of Nafion membranes with polypyrrole has shown high resistance values, composite membrane conductivity may be improved by *in situ* polymerization of a less basic monomer, such as EDOT. The structure of EDOT is shown in figure 4.10.

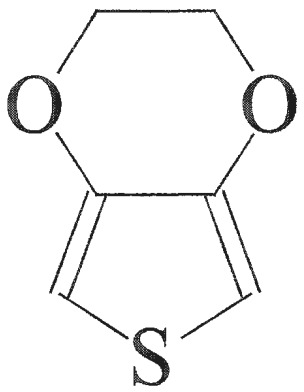

Figure 4.10. EDOT structure.

Two membranes were modified using different oxidants. 20J was modified by H_2O_2 oxidation, while 22J was treated with Fe^{3+}. Figure 4.11 shows the DMFC performances for these poly(EDOT) composite membranes. 20J shows a performance similar to that of Nafion 115; even outperforming it at current densities below 40 mA cm^{-2}. The cell resistance was 0.17 Ω cm^2 which is similar to unmodified Nafion 115, however, surprisingly, the methanol crossover was 154 mA cm^{-2}, which is higher than unmodified Nafion 115.

On the other hand, the resistance of 22J was 0.39 Ω cm^2 and the methanol crossover was 100 mA cm^{-2}. Although the membrane characteristics are similar to 16J, the performance was worse by about 18% at *ca.* 100 mA cm^{-2}.

EDOT, as well as pyrrole, will diffuse into the membrane and fill the pores and decrease the porosity of the membrane. However, the electrostatic interaction between the negatively charged sulfonate groups on Nafion and the positively charged doped form of poly(EDOT) is less than for polypyrrole, since poly(EDOT) is less basic. Therefore, the pores are expected to be bigger in the poly(EDOT)/Nafion membrane, which may increase the membrane's hydration state and enhance its conductivity. However, heavy membrane modification using neat EDOT may affect the ionic cluster structure of the Nafion membrane, and consequently, the composite membrane's properties. Further investigation is required using, for example, diluted solutions for better understanding of the modification procedure.

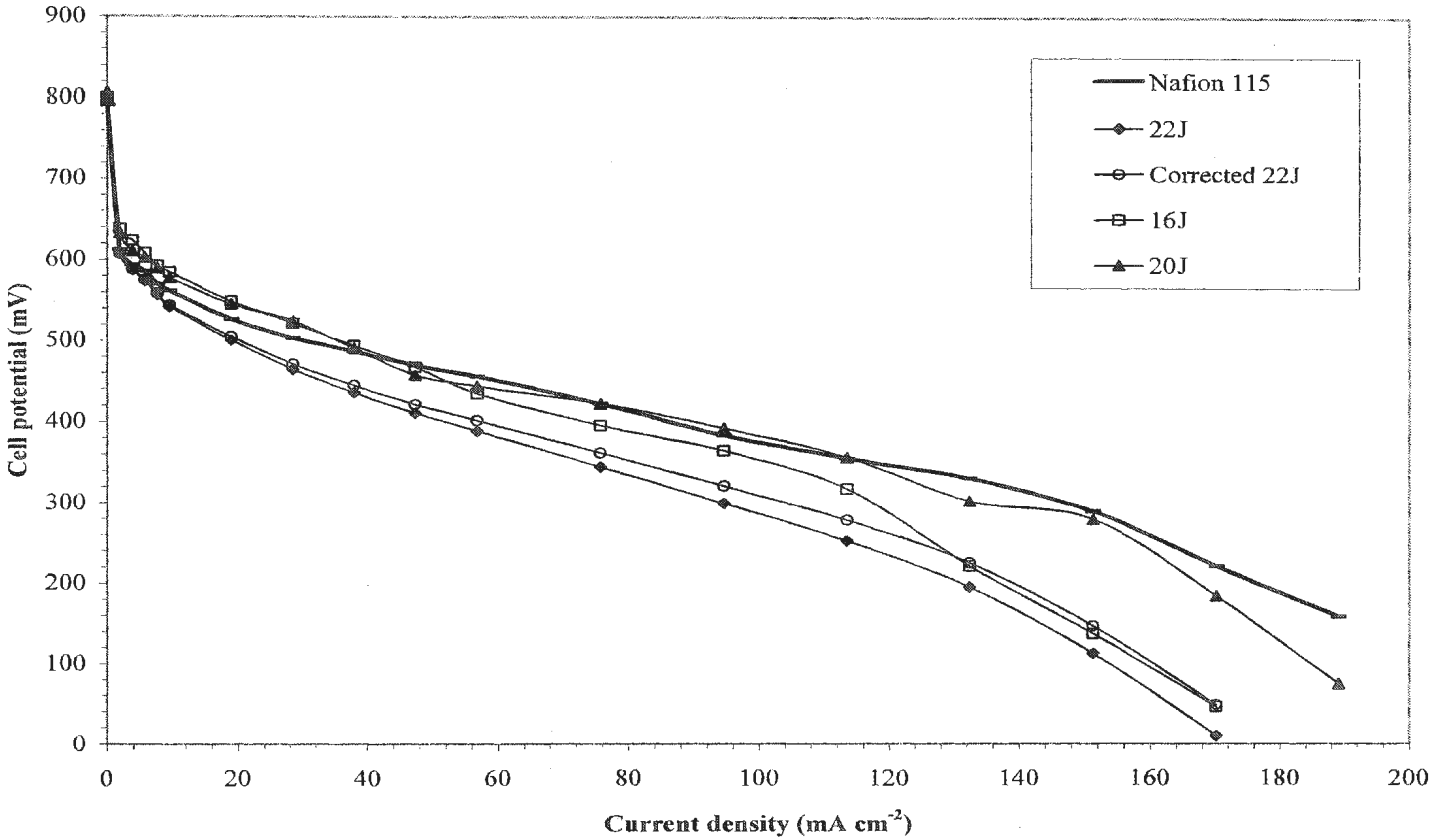

Figure 4.11. DMFC performances for unmodified and modified Nafion 115 running with air at 60 °C and at ambient pressure. f_{air} = 73.1 mL min^{-1}, C_{MeOH} = 1 mol L^{-1}.

4.4 Conclusions

Polypyrrole/Nafion 115 composite membranes have demonstrated excellent performances in a DMFC. In fact, some composite membranes modified by *in situ* polymerization show better performance in a DMFC than untreated Nafion 115 membranes. On the other hand, our results show that the performances of composite membranes are strongly affected by the modification method. Moreover, poly(EDOT)/Nafion composite membranes also show encouraging results.

Although the H_2O_2 modification method shows good blockage of methanol, membrane resistances are variable. However, Fe^{3+} modification can produce membranes with reasonable resistance values but methanol crossover remains too high. Overall, methanol crossover reduction improves the cathode activity and therefore improves the performance of the DMFC.

Figure 4.12 shows the membrane resistance vs I_{lim}^{-1} relationship for most of the membranes reported in this chapter. The best membranes should lie in the shaded region, as they will have lower resistance values with high I_{lim}^{-1}. The best performances were obtained with 2J, JH1028b, BL2-91, 8J, 14J, and 20J, which do lie within this region.

These results suggest that the optimum modification of Nafion should produce a high level of polymeric material inside the membrane and high Nafion to polypyrrole (or poly(EDOT)) character at the surface of the membrane. This would lead to good blocking of methanol (high I_{lim}^{-1} value) and improve the

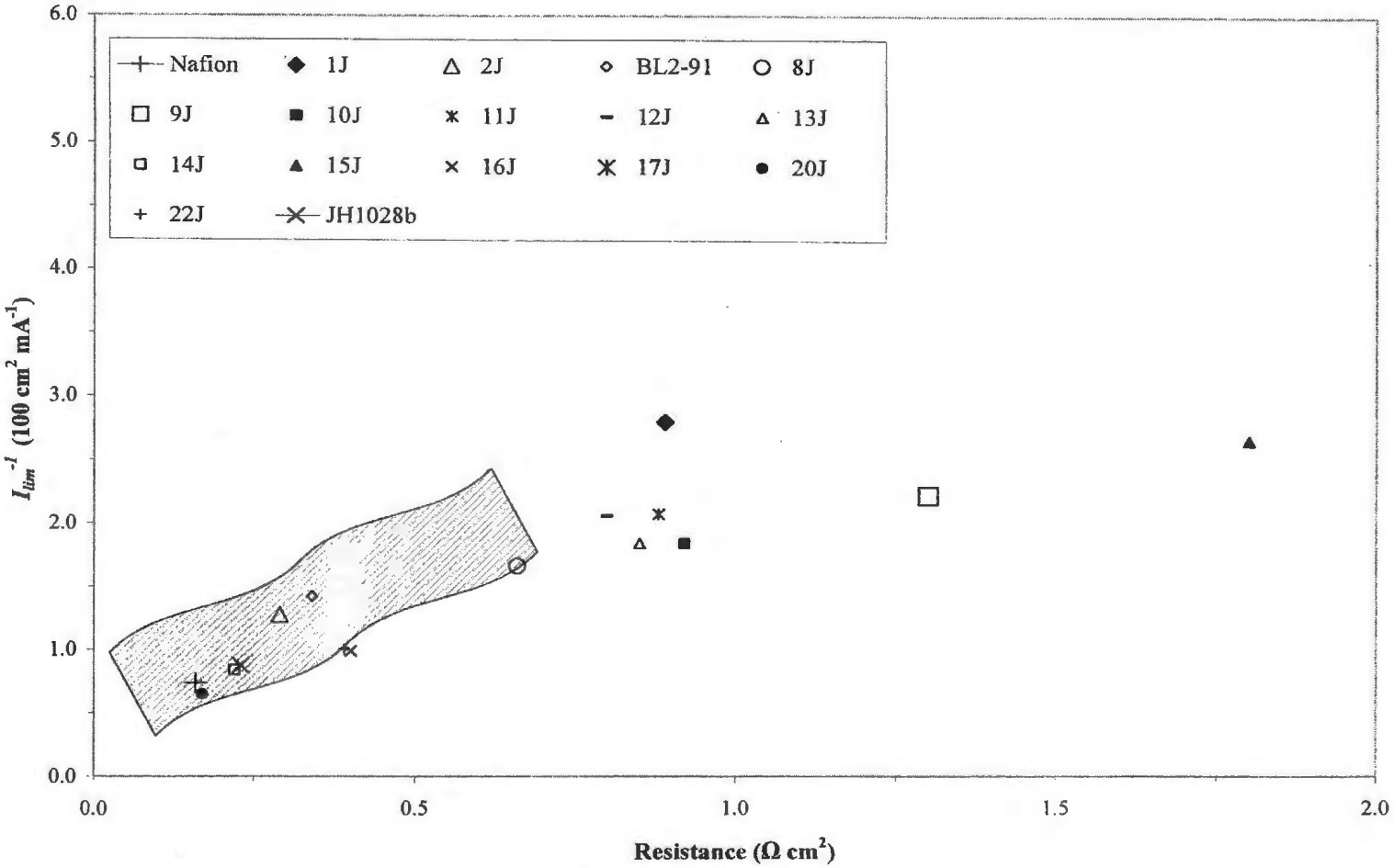

Figure 4.12. Resistance vs. I_{lim}^{-1} diagram for unmodified and modified Nafion 115 membranes.

electrode's cohesion with the composite membrane which may also produce a membrane with a reasonable resistance.

References

[1] Mauritz, K. A.; Stefanithis, I. D.; Davis, S. V.; Scheetz, R. W.; Pope, R. K.; Wilkes, G. L.; Huang, H-H.; *J. Appl. Polym. Sci.* **1995**, 55, 181-190.

[2] Yang, C.; Srinivasan, S.; Arico, A. S.; Creti, P., Baglio, V.; Antonucci, V.; *Electrochem. Solid-State Lett.* **2001**, 4, 4, A31-A34.

[3] Langsdorf, B. L.; Maclean, B. J.; Halfyard, J. E.; Hughes, J. A.; Pickup, P. G.; *J. Phys. Chem. B*, in press.

[4] Jia, N., Lefebvre, M. C.; Halfyard, J.; Qi, Z.; Pickup, P.G.; *Electrochem. Solid-State Lett.* **2000**, 3, 12, 529-531.

[5] E. B. Easton, Ph.D. Thesis, Memorial University of Newfoundland, St. John's, Newfoundland, Canada (2003).

[6] Arico, A. S.; Srinivasan, S.; Antonucci, V.; *Fuel Cells*, **2001**, No. 2, 133-161.

[7] Heinzel, A.; Barragan, V. M.; *J. Power Sources* **1999**, 84, 70-74.

[8] Cappadonia, M.; Erning, J. W.; Niaki, S. M. S.; Stimming, U.; *Solid State Ionics* **1995**, 77, 65-69.

[9] Okada, T.; Xie, G.; Gorseth, O., Kjelstrup, S.; Nakamura, N.; Arimura, T.; *Electrochim. Acta* **1998**, Vol. 43, No. 24, 3741-3747.

[10] Sata, T.; Funakoshi, T.; Akai, K.; *Macromolecules* **1996**, 29, 4029-4035.

[11] Sata, T.; *Chem. Mater.* **1991**,3, 838-843.

Chapter 5

Diagnostics

5.1 Introduction

The cathode and anode activities are very important for DMFC performance. However, slow electro-oxidation of methanol[1,2,3] and the poisoning effect of intermediate species on the Pt surface, especially CO species which are particularly problematic,[4,5] are considered challenging problems. Moreover, methanol permeation from the anode to the cathode decreases the fuel cell performance and poisons the cathode.[6,7,8]

The poisoning effect of CO on the surface of Pt can be minimized by using various Pt-metal alloy catalysts.[9] Many researchers have reported that the best anode catalysts for electro-oxidation of methanol are Pt-Ru bimetallic catalysts.[10,11] These catalysts decrease the methanol oxidation overpotential through a bifunctional mechanism[12] (discussed previously in section 1.5), and therefore enhance the cell performance.

Modification of Nafion® membranes has been utilized to minimize membrane permeation towards methanol.[13,14,15] Composite membranes show less permeability to methanol and therefore improve the activity of the cathode which leads to better cell performance. However, the modification of Nafion membranes has also shown a negative influence on the cell performance, which is unpredicted from thermodynamics or kinetics, and appears to be related to poor bonding to the electrodes.

This chapter reports diagnostic experiments on some of the composite membranes studied in this thesis designed to explain their poor performance and

lead to better understanding.

5.2 Experimental

5.2.1 Anode Polarization Measurements

DMFC anode polarizations were obtained by passing nitrogen with a flow rate of 25.6 mL min^{-1} through the cathode, and with a methanol pumping rate of 0.153 mL min^{-1}. Anode polarization readings were measured as described in section 2.4 for cell polarization measurements. In these experiments, the cathode behaves as a dynamic hydrogen reference electrode (DHE).

5.2.2 Cathode and Anode Cyclic Voltammetry Measurements

Cathode measurements were obtained by, initially, running the DMFC for about 1 hour at room temperature with hydrogen (H_2) at a flow rate of 18.6 mL min^{-1} through the anode and with air through the cathode at a flow rate of 25.6 mL min^{-1}. Then, the cyclic voltammogrames (CV) were obtained, at room temperature, by passing N_2 instead of air through the cathode with a flow rate of 25.6 mL min^{-1}. Anode CVs were obtained by simply switching the gases and electrodes (i.e. H_2 passes through the cathode and air then N_2 through the anode).

In these experiments, the H_2 electrode acts as both a counter electrode and a reference electrode.

5.3 Results and Discussion

5.3.1 Anode Polarization of Composite Membranes

Figure 5.1 shows anode polarizations of composite membranes prepared by H_2O_2 oxidation. BL2-91 and 20J show good anode performance compared to unmodified Nafion 115, and their performance was lower by just 4 and 3% at *ca.* 100 mA cm^{-2}, respectively. However, 8J shows poor performance at 18% lower than Nafion. Its resistance corrected anode performance is better by 12% at the same current density.

The higher resistances of the modified membranes are mainly responsible for the losses in anode performance. However, the 8J corrected anode polarization is still less than expected from resistance differences; this may indicates that 8J's anode has lower active area of the Pt/Ru catalyst than the other membrane's anodes.

On the other hand, the composite membranes prepared or treated with $Fe(NO_3)_3$ solution show different results as shown in figure 5.2. JH1208b demonstrates the best anode performance among these membranes. The anode performances are seen to decrease with increasing membrane resistance and are worse with 9J and 15J, as they have the highest resistances values (1.3 and 1.8 Ω cm^2, respectively).

Resistance corrected anode performances are shown in figure 5.3. As expected from the membrane resistance of JH1208b, its corrected anode

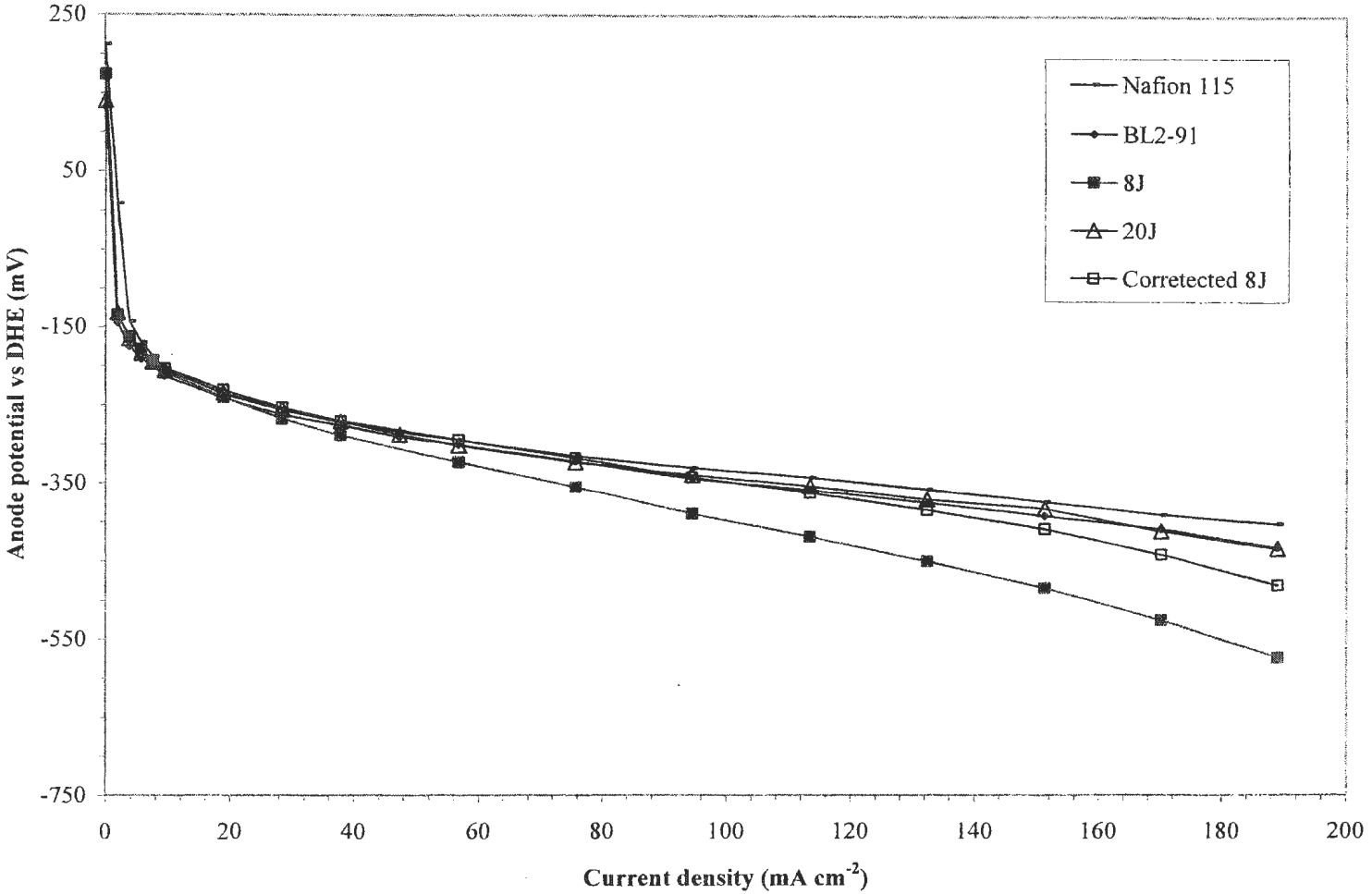

Figure 5.1. Anode performances for unmodified and modified Nafion 115 prepared by H_2O_2 oxidation, running at 60 °C and at ambient pressure. $f_{Nitrogen}$ = 25.6 mL min^{-1}, C_{MeOH} = 1 mol L^{-1}.

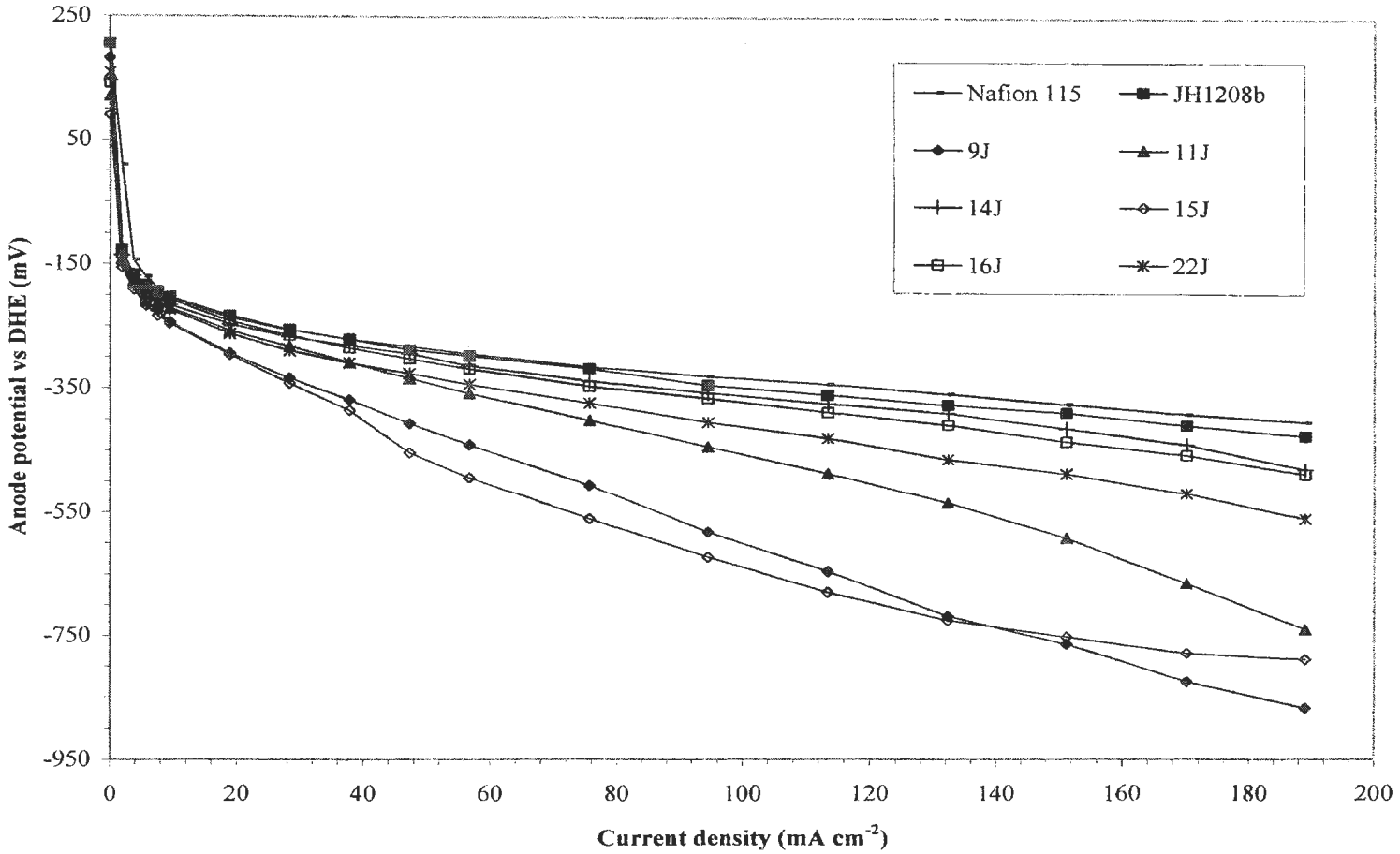

Figure 5.2. DMFC anode performances for unmodified and modified Nafion 115 membranes treated with Fe^{3+} at 60 °C and at ambient pressure. $f_{Nitrogen}$ = 25.6 mL min^{-1}, C_{MeOH} = 1 mol L^{-1}.

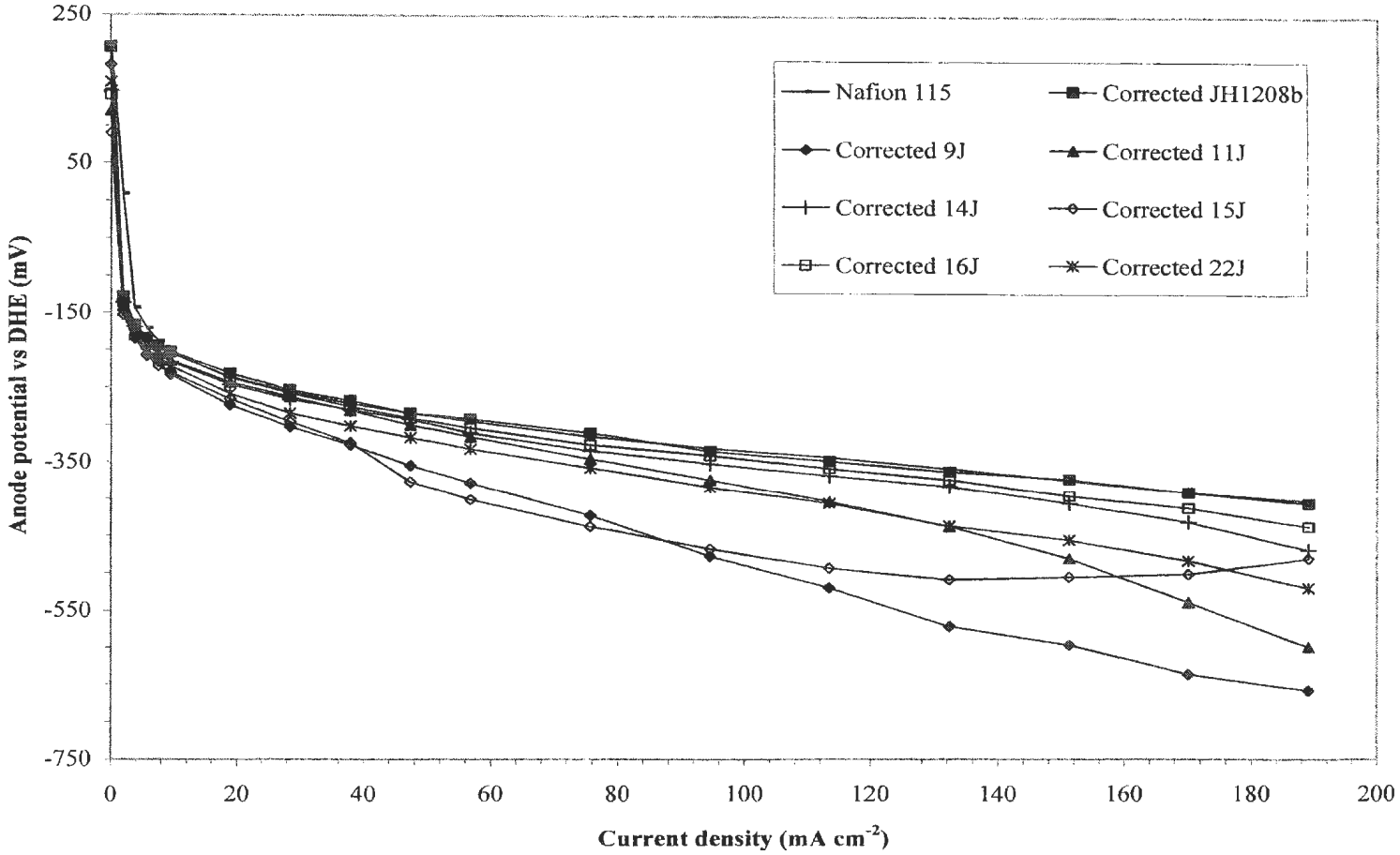

Figure 5.3. Resistance corrected DMFC anode performances for unmodified and modified Nafion 115 membranes treated with Fe^{3+} at 60 °C and at ambient pressure. $f_{Nitrogen}$ = 25.6 mL min^{-1}, C_{MeOH} = 1 mol L^{-1}.

performance overlaps with that of Nafion 115. This indicates that the performance losses are purely Ohmic.

Although the corrected anode performances for the other membranes are improved, the anode performance losses are not parallel with the expectation based on membrane resistances. Poor anode performance is an indication of lower active area of the Pt/Ru catalyst.

All these membranes were modified or treated with Fe^{3+} polymerization. This modification or treatment leads to the formation of a tight layer of polypyrrole at the surface of the membrane[16]. This decreases the Nafion character at the surface of the membrane which therefore inhibits its bonding to the anode. As a result anode delamination often occurs.

Poor interfacial bonding properties reduce the Pt/Ru catalyst utilization and also increase the resistance, which therefore severely reduces the performance. This may explain the lower active area for the composite membranes prepared via the Fe^{3+} method (JH1208b is excluded).

5.3.2 Cathode CVs

CVs of the cathode catalyst for the poorest membrane (9J) were obtained to investigate the effect of modification on cathode characteristics. Figure 5.4 shows the cathode CVs for Nafion 115, and 9J membranes.

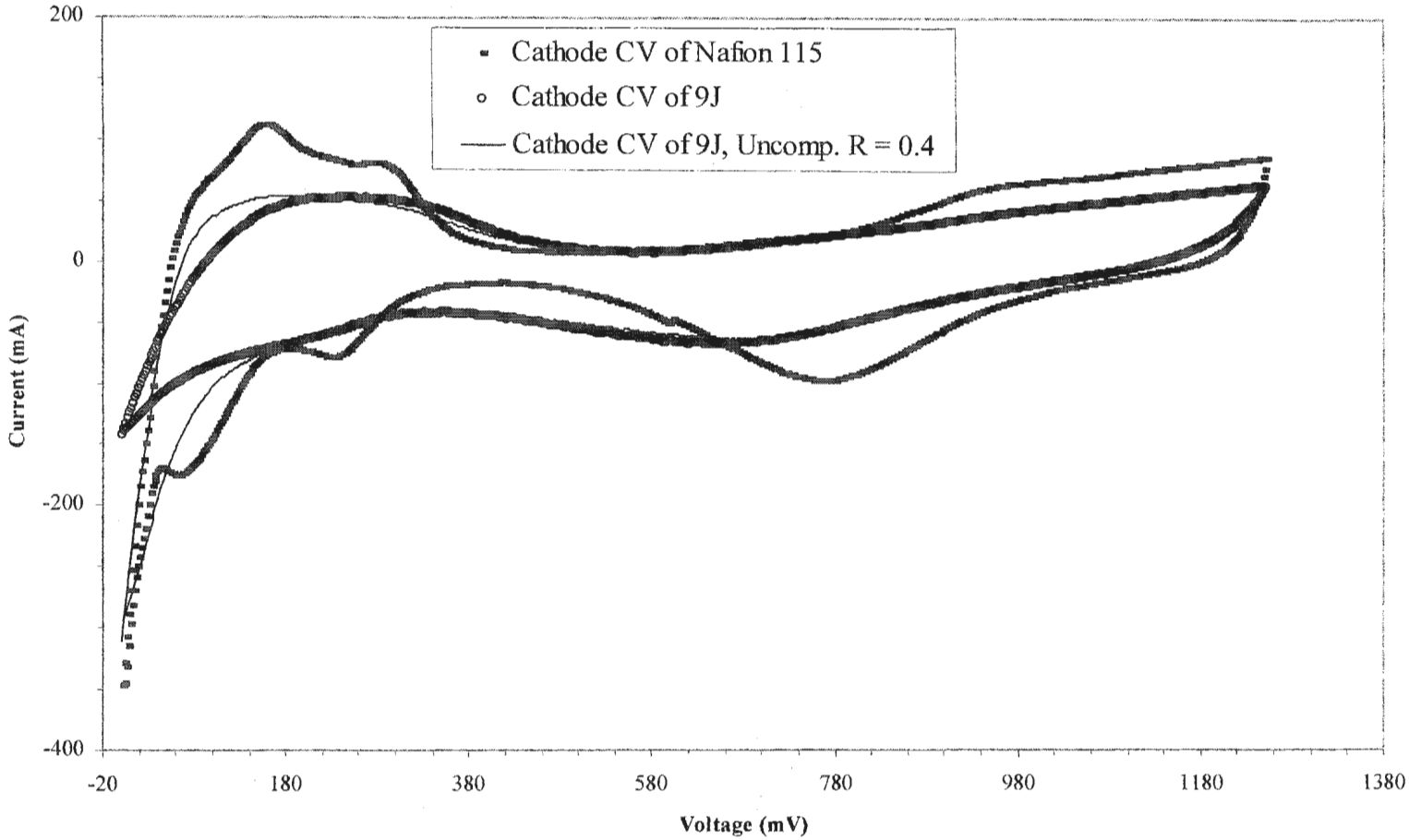

Figure 5.4. Cathode CVs for unmodified Nafion 115 and modified 9J membranes treated with Fe^{3+} at room temperature and at ambient pressure. $f_{Hydrogen}$ = 18.6 mL min^{-1}, $f_{Nitrogen}$ = 25.6 mL min^{-1}, step height = 2 mV, scan time = 0.1 s.

The Nafion 115 cathode exhibits a typical CV for a Pt catalyst. The current peaks in the potential region between *ca.* 20 and 340 mV are attributed to hydrogen adsorption and desorption. The current in the potential region between *ca.* 580 and 1020 mV is due to the oxidation and reduction of the Pt surface.

On the other hand, the 9J cathode exhibits a very poor CV. The hydrogen adsorption/desorption and Pt oxidation/reduction peaks are not well defined and not separated. Moreover, the area under the CV curves is significantly decreased. This indicates that the catalytic activity of the Pt catalyst in the 9J cathode is considerably less than with unmodified Nafion 115, and that the active cathode area is severely decreased with the modified 9J membrane. As a result, a higher cell resistance is observed, and this causes voltage losses and produces poor cell performance. To correct for these Ohmic losses the 9J cathode CV is corrected for the uncompensated resistance using the feature on the potentiostat. Although the corrected CV (figure 5.4) shows some increase in peak areas, it is also poor relative to that for unmodified Nafion.

Poor bonding of the cathode to 9J severely reduces the Pt catalyst utilization and is responsible for lowering the active area of Pt. These results explain the poor cell performance obtained for the modified 9J membrane. Overall, the cathode performances for the composite membranes prepared by the Fe^{3+} method are expected to be poor as a result of poor interfacial bonding properties.

5.3.3 Anode CVs

Figure 5.5 reveals anode CVs for the modified 9J and Nafion 115 membranes. The peaks for Nafion 115 are well defined. However, 9J's anode suffers as well as its cathode from low catalytic activity. Moreover the area under the CV curve is much less than for Nafion 115, which also indicates that the active area of the Pt/Ru anode catalyst is reduced with the modified 9J membrane.

A resistance corrected anode CV was also obtained for 9J (figure 5.5). It shows that the anode performance losses are not just Ohmic. Delamination of the anode from the surface of composite membranes (as described in section 5.3.2) modified by the Fe^{3+} method is responsible for these performance losses.

Poor bonding of the anode to 9J severely reduces the Pt/Ru catalyst utilization and is responsible for lowering the active area of the anode.

5.4 Conclusions

Anode performances as well as cathode and anode CV data obtained for different composite membranes reveal the effect of poor bonding of the electrodes to the surface of the composite membranes on DMFC performance.

Delamination of both electrodes has shown a severe effect on the catalytic activity of the electrodes, which increases the cell resistance and is responsible for a significant reduction of the overall cell performance.

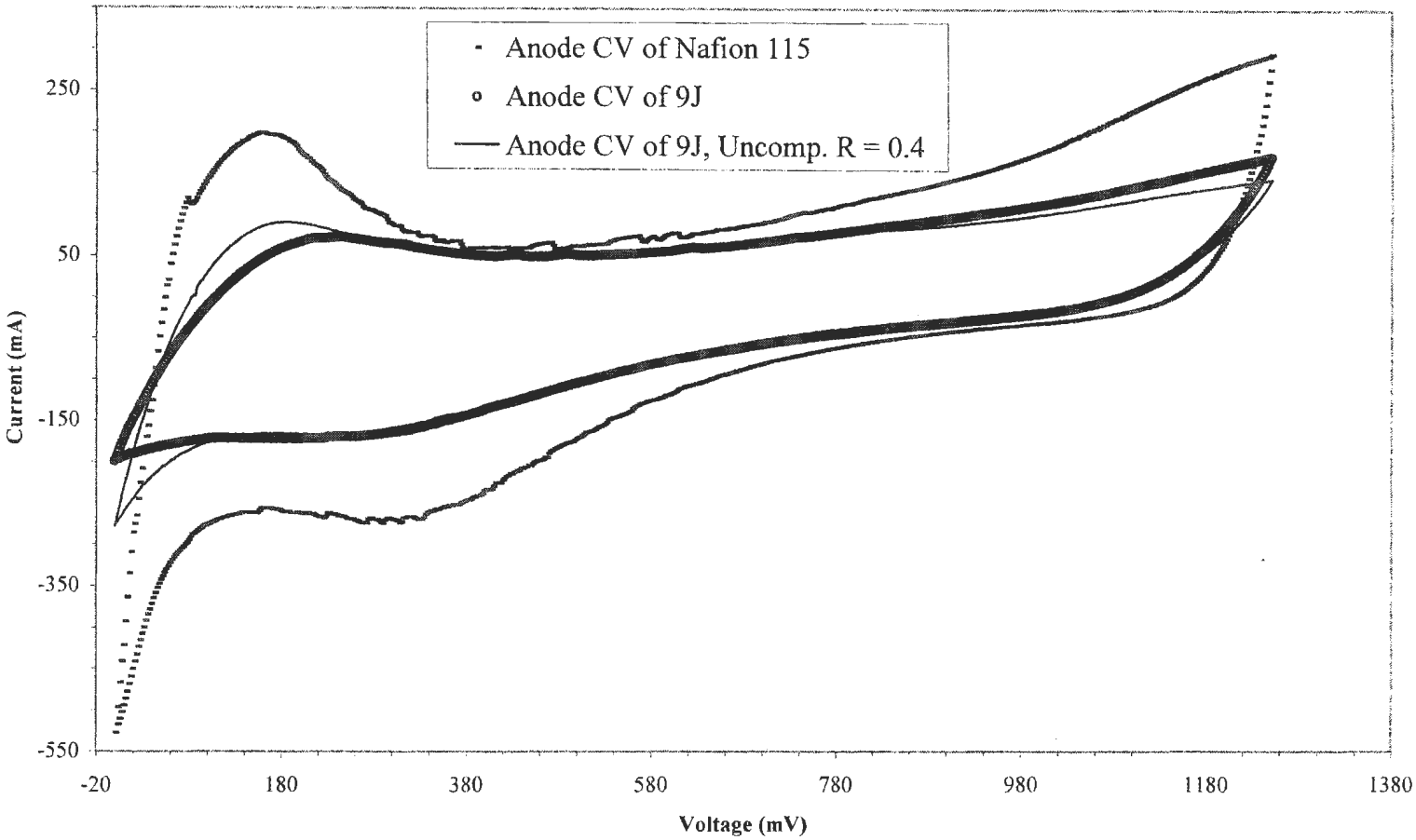

Figure 5.5. Anode CVs for unmodified Nafion 115 and modified 9J membranes treated with Fe^{3+} at room temperature and at ambient pressure. $f_{Hydrogen}$ = 18.6 mL min^{-1}, $f_{Nitrogen}$ = 25.6 mL min^{-1}, step height = 2 mV, scan time = 0.1 s.

References

[1] Jusys, Z.; Behm, R. J.; *J. Phys. Chem. B* **2001**, 105, 10874-10883.

[2] Melnick, R. E.; Palmore, G. T. R; *J. Phys. Chem. B* **2001**, 105, 9449-9457.

[3] Gojkovic, S. L.; Vidakovic, T. R.; *Electrochim. Acta* **2001**, 47, 633-642.

[4] Lamy, C.; Léger, J-M.; Srinivasan, S.; *Modern Aspects of Electrochemistry*, No. 34, Bockris, J. O'M; Conway, B. E., Eds; Kluwer Academic/Plenum Publishers: New York, **2001**, pp 53-118.

[5] Wang, Y.; Fachini, E. R.; Cruz, G.; Zhu, Y.; Ishikawa, Y.; Colucci, J. A.; Cabrera, C. R.; *J. Electrochem. Soc.* **2001**, 148, 3, C222-C226.

[6] Baldauf, M.; Preidel, W.; *J. Power Sources* **1999**, 84, 161-166.

[7] Shao, Z.-G.; Hsing, I-M.; *Electrochem. Solid-State Lett.* **2002**, 5, 9, A185-A187.

[8] Carrette, L.; Friedrich, K. A.; Stimming, U.; *ChemPhysChem* **2000**, 1, 162-193.

[9] Steigerwalt, E. S.; Deluga, G. A.; Cliffel, D. E.; Lukehart; *J. Phys. Chem. B* **2001**, 105, 8097-8101.

[10] Rolison, D. R.; Hagans, P. L.; Swider, K. E.; Long, J. W.; *Langmuir* **1999**, 15, 774-779.

[11] Liu, Y.-C.; Qiu, X.-P.; Huang, Y.-Q.; Zhu, W.-T.; *J. Power Sources* **2002**, 111, 160-164.

[12] Hoster, H.; Iwasita, T.; Baumgartner, H.; Vielstich, W.; *J. Electrochem. Soc.* **2001**, 148, 5, A496-A501.

[13] Yang, C.; Srinivasan, S.; Arico, A. S.; Creti, P., Baglio, V.; Antonucci, V.; *Electrochem. Solid-State Lett.* **2001**, 4, 4, A31-A34.

[14] Langsdorf, B. L.; Maclean, B. J.; Halfyard, J. E.; Hughes, J. A.; Pickup, P. G.; *J. Phys. Chem. B*, in press.

[15] Jia, N., Lefebvre, M. C.; Halfyard, J.; Qi, Z.; Pickup, P.G.; *Electrochem. Solid-State Lett.* **2000**, 3, 12, 529-531.

[16] Sata, T.; *Chem. Mater.* **1991**,3, 838-843.

Chapter 6

Summary

Direct methanol fuel cell (DMFC) characteristics have been studied throughout this thesis. This investigation had led to a better understanding of the fuel cell processes and significantly improved the performance of the DMFC.

The methanol permeability of Nafion polymer electrolyte membranes (PEM) was measured in a DMFC by double-step chronoamperometry. This electrochemical method provides steady state measurements of methanol crossover relatively quickly. Several parameters have been shown to affect the methanol crossover. The results have shown a significant increase in methanol transport through the PEM with increasing temperature, as described by an Arrhenius type relationship.

Methanol crossover is roughly inversely proportional to membrane thickness. A 50% reduction in methanol crossover was obtained by increasing the thickness from 51 (Nafion 112) to 178 (Nafion 117) μm, using 1 mol L^{-1} methanol at 60 °C.

The concentration influence on methanol permeation has been also explored. It has been found that methanol diffusion increases linearly with increasing concentration of methanol. Although this results in fuel losses in a DMFC, the best DMFC performance was obtain with 1 mol L^{-1} methanol.

Modification of the Nafion PEM with polypyrrole has shown a significant effect on DMFC performance. The composite membranes improve the fuel efficiency of the DMFC by decreasing methanol crossover. However, their properties and performances are strongly affected by the modification method.

Composite membranes prepared by Fe^{3+} oxidation of pyrrole show reasonable resistance values but their methanol permeation is often still too high. Most of these membranes produce poor DMFC and anode performances, which are related to poor bonding of the electrodes with the modified membrane's surface.

On the other hand, H_2O_2 modification produces composite membranes with good blockage of methanol. The resistance of these membranes, however, was variable and affected by the modification procedure.

Some polypyrrole/Nafion composite membranes have shown excellent DMFC performance. Membranes prepared via the two modification methods have outperformed unmodified Nafion 115 by 7 and 11%, respectively. The performance gains with the composite membranes are due to better cathode activity as a result of methanol crossover reduction. Poly(EDOT)/Nafion composite membranes also show encouraging results.

Cyclic voltammetry (CV) of the cathode and the anode with one of the worst membranes were investigated. The result show poor cathode and anode CV's, and low active catalyst areas. This is primarily a result of poor bonding of the electrodes with the membrane, which causes delamination. This has shown a severe effect on the catalytic activity of the electrodes, which increase the cell resistance and is responsible for a significant reduction in the overall cell performance.

It can be concluded that the optimum modification of Nafion membranes should have a high level of polymeric materials inside the membrane and high Nafion to polymer character at the surface of the membrane. This modification is expected to produce composite membranes with good blocking of methanol and improve bonding of the electrodes with the membrane surface.

The conductivities of the modified membranes may be improved by using a less basic monomer. Nafion modification with poly(EDOT) has shown reasonable resistance values compared to pyrrole, however, further investigation is required.